Characteristics of sediments and regolith alterations in the Plio-Pleistocene succession, coastal cliff sections, St Vincent Basin, South Australia

Richard May[1] & Anthony Milnes[2]

[1]Formerly at Department of Soil Science, The University of Adelaide, South Australia, Australia

[2]Department of Earth Sciences, The University of Adelaide, North Terrace, Adelaide 5005, South Australia

Anthony Milnes https://orcid.org/0000-0003-4283-4428

Correspondence concerning this article should be addressed to Dr Anthony Milnes, Department of Earth Sciences, The University of Adelaide, North Terrace, Adelaide 5005, South Australia. anthony.milnes@adelaide.edu.au

Short title: St Vincent Basin Plio-Pleistocene, South Australia

Abstract

Syn- and post-depositional alterations are distinguished in a detailed lithological and mineralogical study of the largely unconsolidated Plio-Pleistocene non-marine succession in coastal cliff sections in the St Vincent Basin south of Adelaide. At its base, the sequence interfingers with Late Pliocene estuarine marine sediments in places but mostly unconformably overlies older Cenozoic marine sediments or Neproterozoic bedrock. The fluvial and alluvial siliclastics have bioturbation, blocky-prismatic macro-peds and subtle Fe-mottling indicators of hiatuses in deposition, and imprints of soil and shallow groundwater environments. A relative abundance of kaolinite, illite and randomly interstratified illite-smectite reflects both sediment source and conditions in the local depositional environment. A thick deposit of aeolian calcareous silt with associated pedogenic calcretes blankets the succession. Conspicuous bleached Fe mega-mottled intervals and zones of alunite-halloysite within the sequence record post-depositional, groundwater-related alterations in regolith environments. These formed during incision and erosion of the sedimentary fill in the basin in response to regional falls in base level. Each marks a different time and specific geomorphic environment according to the chemistry of the discharge of local groundwaters from aquifers that were intersected by incision and scarp retreat.

Lay Summary

Excellent exposures of Plio-Pleistocene non-marine sediments in sea-cliffs in the St Vincent Basin in South Australia provided an opportunity to review the stratigraphic succession, determine the composition of the sediments, and distinguish depositional features from distinctive later regolith overprints. Early siliclastic fluvial and alluvial sedimentary environments were later replaced by an aeolian and pedogenic carbonate system which blanketed large areas of the landscape. Subsequent erosion triggered by falls in base-level generated weathering environments in which conspicuous bleaching/iron-mottling and alunite/halloysite alteration occurred in specific zones and at different times in response to outflow of local chemically distinct groundwaters.

Keywords: Plio-Pleistocene; Non-marine; Sedimentology; Mineralogy; Regolith.

1. Introduction

The modern sea cliffs bounding St Vincent Gulf in South Australia display excellent sections through the Cenozoic marine and overlying non-marine sedimentary fill in the St Vincent Basin (Figure 1; Stuart 1969; McGowran & Alley, 2008). St Vincent Basin is ~15,000 km^2 in area, underlies St Vincent Gulf, and is defined by a series of roughly N-S arcuate early Palaeozoic faults that were reactivated in the Late Palaeogene as the separation of Australia and Antarctica progressed. A compressional tectonic regime which formed the basin in Proterozoic, Cambrian and Carboniferous-Permian bedrock, and also generated sub-basins or embayments (asymmetrical tectonic valleys) including the Willunga Embayment, Noarlunga Embayment, and Adelaide Plains Sub-basin, was responsible for periodic disruption of sedimentation and later uplift of the adjacent highlands of Fleurieu Peninsula (Figure 1; McGowran & Alley, 2008; McGowran et al., 2016; Preiss, 2019b). The earliest deposits are non-marine middle Eocene sediments overlain by marginal marine and marine limestones ranging in age up to the late Pliocene (Stuart 1969; Cooper, 1985; McGowran et al., 2016). From the late Pliocene onwards the seas regressed, and terrestrial fluvial and alluvial sediments progressively filled the basin.

The Plio-Pleistocene sediments, which are largely unconsolidated in contrast to the underlying marine sequence, are well-exposed in sea cliffs (Figure 2) cutting through the Noarlunga and Willunga Embayments. These are the southernmost of several asymmetric fault-angle depressions along the eastern margin of the basin, with their deeper southern margins against the bounding Ochre Cove-Clarendon and Willunga Faults, respectively (Figure 3). The cliffs are commonly more than 20 m high and typical of active erosion on many coasts around the gulf. There are also abandoned cliffs backing shallow embayments marking former higher sea-levels, and bathymetric evidence of cliffs offshore, particularly on the western side of the Gulf (Bye & Kampf, 2008; Figure 5.1 in Richardson et al., 2005), corresponding to the coasts of former low sea-levels. The morphology of the cliffs changes according to lithology and structure, as well as the nature of the beach: near-vertical forms are typical of cliffs that have formed in indurated Cenozoic marine limestones, whereas inclined slopes usually characterise the unconsolidated non-marine Plio-Pleistocene sediments. Where beaches are narrow, erosion due to wave action, high tides and storm surges is active and steep cliffs are maintained as back-wearing progresses. Where beaches are wide, wave and tide energies are dissipated, active marine erosion is reduced, subaerial processes become important, and cliff slopes are flattened (Hampton et al., 2004). To date there has been no systematic study of the development of the seacliffs in the study area, although it is generally accepted that they register a complex interaction between initial fluvial incision of the Plio-Pleistocene fill in the basin and later episodic marine erosion as sea levels fluctuated.

Broadly, the Plio-Pleistocene sequence consists of fluvial and alluvial sediments at the base, an intermediate thick and extensive clay unit topped by fluvial sands, and an uppermost widespread blanket of aeolian carbonate silt and pedogenic calcrete mantled by modern soils. Overprinting the primary features of the sediments in the cliff exposures are a general but variable reddening/yellowing due to iron oxide colourations, various forms of pedality in the clays, evidence of bioturbation, horizons with carbonate mottling, both subtle and conspicuous iron-mottling and bleaching, and seams of alunite and halloysite.

There have been various stratigraphic subdivisions proposed for the Plio-Pleistocene sediments in the coastal cliffs around Gulf St. Vincent but, other than the detailed studies by Sheard and Bowman (1994) of soils and near-surface sediments in the Adelaide Plains Sub-basin, there is no record of the detailed character of the sediments, and no basin-wide study of the succession.

Together with companion research by Phillips (1988), this investigation focusses on a re-examination of the Plio-Pleistocene succession exposed in the sea-cliffs in the area studied by Ward (1966). Detailed lithostratigraphic observations were recorded and sedimentological, mineralogical and selected chemical analyses made following the systematic sampling of four cliff sections: another eight sections were studied in less detail. The main objectives of this study are to critique prior interpretations of the nature of the succession, and to document the secondary alterations, the most distinctive of which have an origin in regolith environments rather than depositional environments as assumed by others.

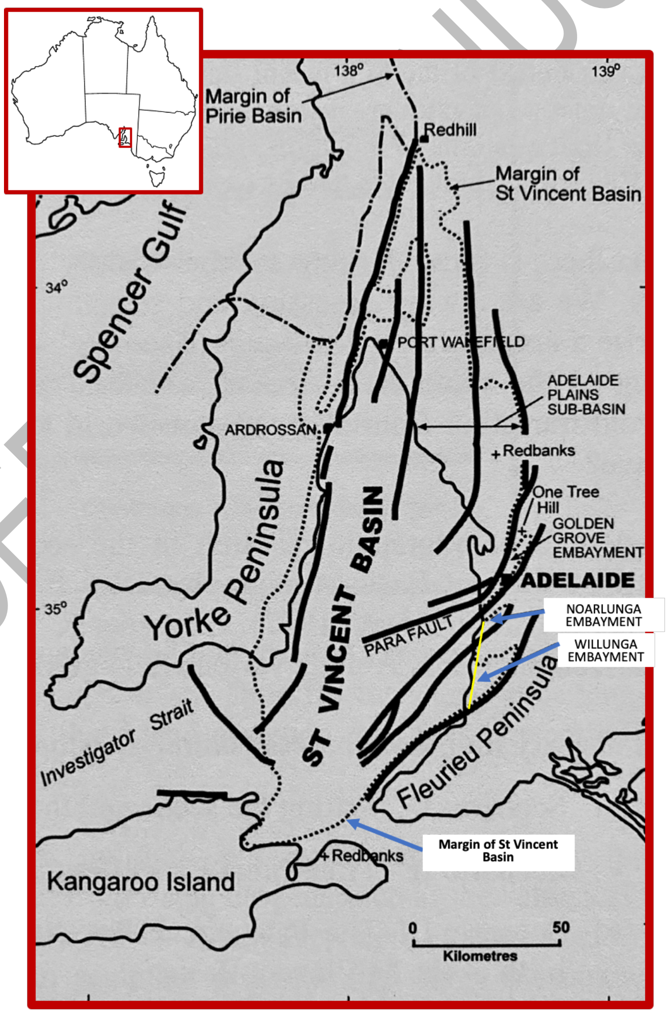

Figure 1. Map showing location of Willunga & Noarlunga Embayments on the eastern margin of the St Vincent Basin (from McGowran & Alley, 2008). Heavy lines represent Cenozoic fault traces. Inset shows regional location. Yellow line locates the transect in Figure 3.

Figure 2. Typical sea-cliffs in the Willunga and Noarlunga Embayments where unconsolidated vari-coloured Plio-Pleistocene non-marine sediments overlie off-white indurated Eocene-Pliocene marine limestones (Google Earth views). (A) Maslin Bay, north of Blanche Point; (B) Onkaparinga River mouth; (C) Port Willunga, looking southeast; (D) Sellicks Beach. Site locations in Figure 3. (A), (B) & (C) – vari-coloured clay formation is prominent; (D) – basal sand-gravel formation is prominent.

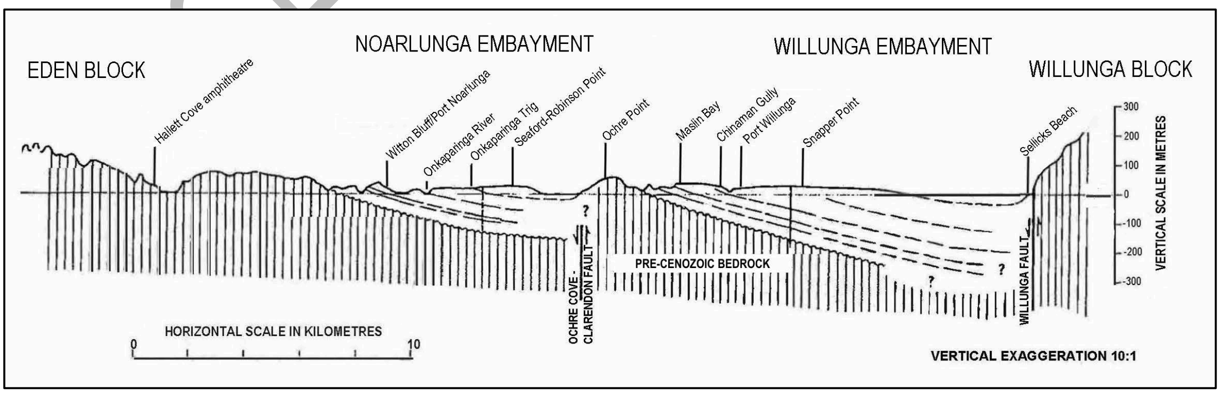

Figure 3. N-S coastal transect (yellow line in Figure 1) across the Noarlunga & Willunga Embayments showing locations of studied sections in relation to the geology (modified from McGowran et al., 2016). Trend-lines in embayments represent bedding in Cenozoic sediments; vertical lines represent Neoproterozic bedrock.

2. Methods

Coastal cliff exposures between Hallett Cove and Sellicks Beach (Figure 3) were mapped in a reconnaissance fashion. Particular attention was paid to lithologies, lateral facies distribution, and distinctive sedimentological, mineralogical and alteration features. Some samples were collected for laboratory analyses to aid in the selection of key sections for detailed study. Four sections at Snapper Point, Maslin Bay, Onkaparinga Trigonometrical Station (Onkaparinga Trig) and Hallett Cove were ultimately chosen: another eight sections were examined in less detail. Bulk samples (0.5-1 kg) were collected systematically at 50 cm intervals vertically through sections at each of the four key sites: additional samples were collected where interesting features or frequent lithological changes were noted. Sampling commenced immediately above the unconformity at the base of the Plio-Pleistocene sequence and terminated just below the ubiquitous regional carbonate blanket (the subject of a companion study by Phillips, 1988). Descriptions were made of each sample and its relationship with surrounding sediments.

Because the sediments are mostly unconsolidated (somewhat indurated horizons limited to zones of secondary alteration), samples were analysed by means of standard and well-established soil science techniques in the Soil Mineralogy laboratories at CSIRO Division of Soils and the University of Adelaide Department of Soil Science, Adelaide. Samples were disaggregated and dispersed so that their particle size composition could be measured. Specific size fractions were separated for mineralogical analysis (including clay mineral identification, abundance and crystallinity): some were analysed for major and minor element composition. Mineral identifications were made by X-ray diffraction (XRD); major and minor element compositions were made by X-ray fluorescence (XRF). Clay minerals in oriented samples of <2 μm particle size fractions were identified after various treatments including Mg-saturation, glycerolation, K-saturation and heating. Semi-quantitative determinations of the abundances of the various clay mineral constituents were based on cation exchange measurements in conjunction with diffraction peak intensities. All sample preparation and analysis techniques are detailed in the Supplement Section 1 (https://doi.org/10.6084/m9.figshare.25951666): all were undertaken by the lead author during PhD studies in the late 1980s and early 1990s.

3. Makeup of the Plio-Pleistocene succession

3.1. Lithology, sedimentology and mineralogy

Lithostratigraphic mapping of the four key sections and eight subsidiary sections in the coastal cliffs confirmed an initial assessment that the Plio-Pleistocene succession presents as four distinct superposed intervals; a basal sequence of sands, clays, grits and gravels; a prominent clay interval; an upper unit of sands with clays; and a 'blanket' of carbonate silts and calcretes unconformably overlying the regional geology. The latter is a complex formation described separately and in detail by Phillips (1988) and Phillips & Milnes (1988) and was not part of the current investigations. Annotated diagrams of the key sections, together with graphs of particle size and mineralogical distributions, are given in Figures 4-7[1]: Figure 8 is a selection of field photographs (additional photographs are in the Supplement Section 4).

3.1.1. Basal interval of sands, clays, grits and gravels

3.1.1.1. Maslin Bay

At the base of the Plio-Pleistocene succession there is a 1 m interval of grey-green sandy clay with abundant large, soft carbonate mottles that are commonly dolomitic, and frequently coalesce into large masses (Figure 4). This interval is assigned to the Late Pliocene Burnham Limestone (Ludbrook, 1983; Beu, 2017), a soft, friable marl with a rich marine fauna including the holoplanktonic gastropod *Hartungia dennanti chavani* (=*Janthina typica*) which defines its Pliocene age (Beu, 2017). A yellow to orange sand up to 1 m thick overlies it. Immediately above is a thin layer of grey-black manganese oxide impregnating the sandy sediment. Between 2-4 m above the mottled carbonate interval there are several sand bands containing halloysite in the form of grey, waxy bulbous masses. Thin, elongate pods of white alunite are also present. A 1.5 m thick interval of indurated sand and silt about 5.5 m above the mottled carbonate contains large, red, vertically-oriented hematite mottles. Mega-mottled intervals like this are persistent along strike but there are similar intervals in other stratigraphic positions within the sequence: the intervening sandy clays and clays are not mottled. Grey-white sands to about 13.5 m have a sharp upper contact with massive grey-green clays that mark the base of the overlying interval.

The particle-size distribution (data tabulated in Supplement Table 3.1) shows a considerable variation in the basal 2 m of section as a result of secondary alteration and induration by alunite, halloysite, dolomite, and manganese oxide. This caused difficulties in effectively disaggregating the sediments and dispersing the framework constituents. In fact, meaningful particle size data could not be obtained for the conspicuous Fe mega-mottled horizon 6.5-7.5 m above the base of the section. Particle-size data for the overlying grey-white sands with minor Fe mottles are typical for silty sands with about 25% clay.

Heavy mineral (SG>2.96) concentrates in the >250 μm sand fractions of two samples from below the Fe mega-mottled horizon and one from within it are dominated by tourmaline, sillimanite, iron oxides and staurolite (Table 1).

[1] Detailed data tables, together with descriptions and annotations of the subsidiary sections, are in the Supplement Section 2 at https://doi.org/10.6084/m9.figshare.25951666

Table 1. Mineralogy of heavy mineral concentrates in coarse sand fraction of Maslin Bay samples.

Sample number	RM259	RM262	RM265
	Basal sands interval		
Iron oxides	0.1-1%	20-50%	1-3%
Tourmaline	20-50%	20-50%	20-50%
Sillimanite	20-50%	3-10%	20-50%
Staurolite	3-10%	1-3%	1-3%
Garnet			
Rutile	2-10 grains	2-10 grains	2-10 grains
Mica			
Ilmenite			
Kyanite		0.1-1%	3-10%
Barite			
Zircon			2-10 grains
Amphibole			
Spinel			
Corundum			
Andalusite	2-10 grains	1 grain	
Rock fragments		10-20%	0.1-1%
Leocoxene			0.1-1%

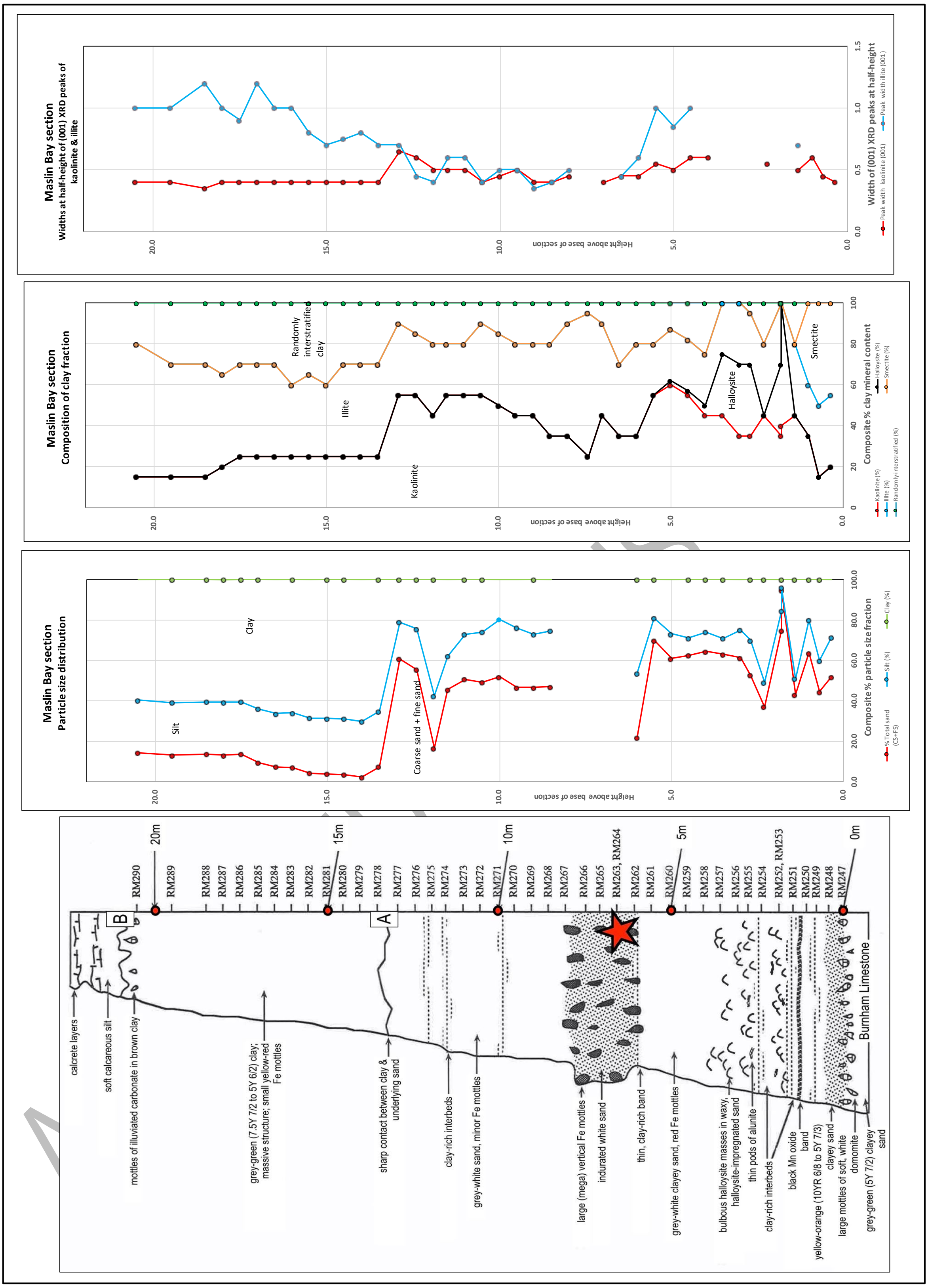

Figure 4. Annotated lithology, particle size composition, and mineralogy of the Plio-Pleistocene succession in the Maslin Bay section, northern Willunga Basin. Red dots at right are 5 m intervals from the base of the succession set at 0 m; dashes indicate sample locations and numbers. All data tabulated in Supplement Table 3.4. A = top of the basal interval; B = top of the overlying prominent clay interval. Red star = Fe mega-mottle sample.

In terms of the clay fraction, smectite and halloysite are major components in the zones of secondary alteration in the bottom 5 m of the basal formation (Figure 4; Supplement Table 3.1). At the base of the section three samples contain up to 50% smectite with subordinate illite and kaolinite. Above this, in the sand interval between 1.8 and 5 m, there is a significant concentration (~30-40%) of halloysite (but no smectite) together with kaolinite, illite and subordinate randomly interstratified clay. The indurated Fe mega-mottled sand from 6.5-8.0 m is enriched in illite relative to kaolinite and depleted in interstratified clay. The clays in overlying grey-white sands with clay interbeds are dominated by kaolinite. Although data is sparse, illite is highly disordered in the zone of secondary alteration at the base of the interval where kaolinite also has broadened XRD peaks.

Minor amounts of quartz occur in most of the <2 µm clay fractions with feldspar a common component (Supplement Table 3.1). Goethite is a minor component in smectite-containing samples from the base of the formation and in one sample at the base of the iron-mottled zone.

3.1.1.2. Onkaparinga Trig

Up to 20 m of the Plio-Pleistocene succession overlies a karst surface on the Oligo-Miocene Port Willunga Formation at Onkaparinga Trig (Figure 5). The basal part of the interval is a thin green-yellow clay immediately overlying the limestone and infilling karst hollows. It contains small, rounded masses of soft, chalky alunite with thin, elongate pods of alunite up to 3 cm thick and 25 cm long in the overlying 1.3 m of interbedded sand and sandy clay (Figure 8H). Rounded, waxy halloysite-rich pods up to 15 cm across are also present. A 10 cm thick band of yellow-brown sand cemented by iron oxides (dominantly goethite) overlies the halloysite horizon and this is, in turn, overlain by pink and white, unconsolidated fine sands. Several gravel units containing sub-angular to sub-rounded clasts of quartz, quartzite, siltstone and weathered schist (0.5 to 2 cm in size) occur in the succeeding 3 m and grade upwards into fine micaceous sand and silt to around 6 m where the top of the interval is marked by a sharp contact with the overlying clay.

In terms of particle size, there are considerable variations in sand and clay but very little silt in the basal interval: some units contain more than 60% sand whilst others up to 50% clay[2].

Kaolinite, illite, smectite, halloysite and interstratified clays occur in the clay fractions of samples throughout the section (data tabulated in Supplement Table 3.3). Both smectite and halloysite were only found in the basal sands interval but not together: halloysite occurs in two samples of sandy interbeds in the bottom 3 m with minor illite and a trace of randomly interstratified clay; randomly interstratified clay occurs together with illite and kaolinite in samples immediately underlying and overlying the halloysite; smectite is confined, together with illite and kaolinite, to the overlying silty sands and up-section to the sharp contact with the overlying clay interval. Illite and kaolinite appear to be equally well-ordered in intervals above the secondary alteration.

[2] Note that sand and silt concentrations were not determined in some samples.

The composition of a heavy mineral concentrate from the >250 µm particle-size fraction from one sample (RM304) of the basal interval, a red-grey sandy clay, is dominated by barite and mica with accessory iron oxides and staurolite (Supplement Table 3.4).

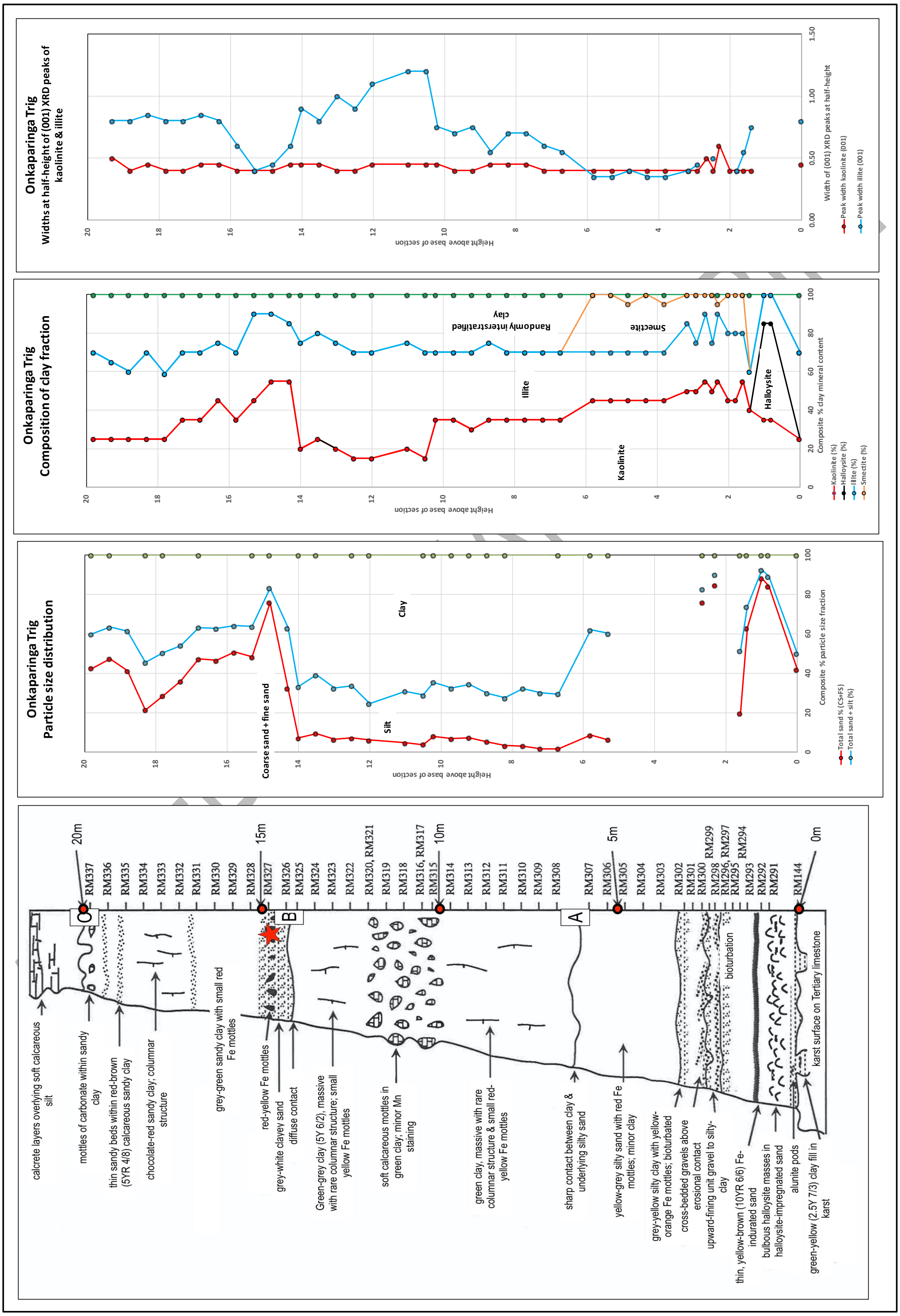

Figure 5. Annotated lithostratigraphy, particle size composition and mineralogy of the Plio-Pleistocene succession in the Onkaparinga Trig section, Noarlunga Basin. Red dots at right are 5 m intervals from the base of the succession set at 0 m; dashes indicate sample locations and numbers. All data tabulated in Supplement Table 3.1. A = top of the basal interval; B = top of the overlying clay interval; C = top of the uppermost sand interval. Red star = Fe mega-mottle sample.

3.1.1.3. Hallett Cove

In our sampled section in the Hallett Cove amphitheatre (Figure 6), the basal interval overlies unconsolidated Permian sediments. This interval consists of grey-green, horizontally-bedded sand with minor gravel lenses containing sub-angular clasts of quartz, siltstone, sandstone and ferruginous material. Grey-green to yellow clays or sandy clays, which tend towards red-brown colours, continue upwards for 3 – 4 m underlying a thick, sandy to silty and indurated horizon in which there are prominent, vertically-oriented Fe mega-mottles (Figure 8B). Laterally, ~70 cm of grey-green sandy clays with thin gravel beds overlie a thin remnant of the Pliocene marine Hallett Cove Sandstone (Glaessner & Wade, 1958; Ward, 1966; Stuart, 1969). In some places, these sandy clays contain a discontinuous zone of mottled, white carbonate in the upper 15 cm, pointing to an interfingering relationship with what is probably a lateral extension of the Late Pliocene marginal marine Burnham Limestone. About 4 m of sands and sandy clays with rare gravel beds and thin clay bands above the mega-mottled interval mark the uppermost part of the interval where there is a sharp, undulating contact with the overlying clay interval.

The indurated Fe mega-mottled horizon between 5-8 m above the base of the section could not be disaggregated effectively and so its particle size composition could not be determined, although clay-sized material was available for analysis. The green-grey interval below the distinctive Fe-mottled horizon is essentially a clayey silt (more than 60% <2 µm material with ~20% silt) but becoming sandier up-section (Figure 6). Above are sandy clays (with >50% sand).

No secondary alteration in the form of halloysite or smectite was identified in the amphitheatre section. The <2 µm fraction of the sandy clay at the very base of the basal interval contains up to 40% randomly interstratified clay, exceeding the abundance of both illite and kaolinite (data tabulated in Supplement Table 3.5). Above, through the green-grey clay and into the Fe-mottled horizon, the concentrations of kaolinite and illite progressively increase at the expense of randomly interstratified clay. The Fe mega-mottled interval itself is dominated by kaolinite and illite with only minor interstratified clay, which is likely to be a consequence of the secondary alteration process. With the exception of a grey sand with small red-brown ferruginous mottles near the top of the interval, in which some hydroxy-interlayered smectite occurs, all interstratified clays were identified as interlayered illite and smectite. The smectitic component is mostly in the range 20 - 30% but in some samples increases to 40-50%.

From the point of view of crystallinity, kaolinite displays some peak broadening. The accompanying illite is significantly disordered in the basal sand horizon as well as in a distinct interval about 3 m above the base where kaolinite, as well as being more abundant than illite, is also disordered (Figure 6).

Minor amounts of quartz are present in the <2 µm fraction of all samples from the Hallett Cove section, with feldspar noted in about half of the samples from the basal interval (Table 3.5 in Supplement).

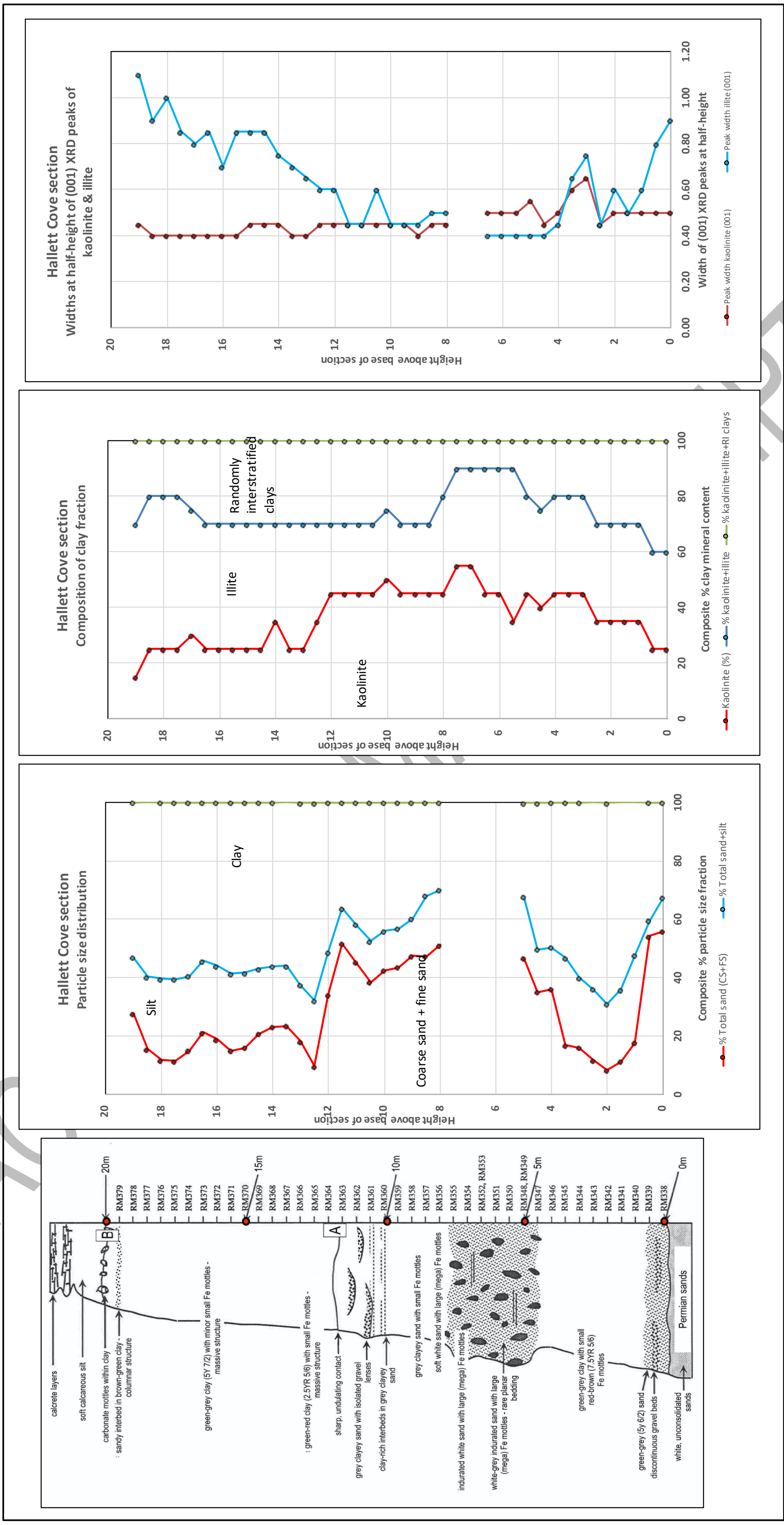
Hallett Cove section
Widths at half-height of (001) XRD peaks of kaolinite & illite
Height above base of section
Width of (001) XRD peaks at half-height
Peak width kaolinite (001)
Peak width illite (001)
Hallett Cove section
Composition of clay fraction
Randomly interstratified clays
Illite
Kaolinite
Composite % clay mineral content
Kaolinite (%)
% kaolinite+illite
% kaolinite+illite+RI clays
Hallett Cove section
Particle size distribution
Clay
Silt
Coarse sand + fine sand
Composite % particle size fraction
% Total sand (CS+FS)
% Total sand+silt
20m
15m
10m
5m
0m
Permian sands

100

Figure 6. Annotated lithostratigraphy, particle size composition and mineralogy of the Plio-Pleistocene succession in the Hallett Cove amphitheatre, Noarlunga Basin. Red dots at right are 5 m intervals from the base of the succession set at 0 m; dashes indicate sample locations and numbers. All data tabulated in Supplement Table 3.3. A = top of the basal interval; B = top of prominent clay interval.

3.1.1.4. Snapper Point

The basal interval of sands, grits and gravels is not recognised in the Snapper Point section.

3.1.2. Prominent clay interval

The middle interval in the Plio-Pleistocene succession is dominantly clay with a self-mulching surface which effectively obscures any primary sedimentary structures. Typical sections feature a massive, red to grey-green clay with rare thin (~1 mm) laminae of fine sand near the base. Where exposed, the contact between the clay and the underlying sand interval is everywhere sharp.

3.1.2.1. Maslin Bay

Here, massive grey-green clays of the prominent clay interval occupy the upper 9 m of the sampled section (Figure 4) and are overlain by the carbonate blanket consisting of several metres of calcareous silt capped by calcrete. The uppermost sand and clay interval in the succession is absent.

There is a clear distinction between the basal sand interval and the overlying prominent clay interval based, in the first instance, on the particle size distribution (Supplement Table 3.1). A sand horizon immediately underlies the clay interval which consistently has up to 70% clay at the base of the unit, reducing to ~60% from about 17.5 m up to the carbonate blanket at 20.5 m. The silt content is consistently around 12%, but the sand content is very low at the base increasing to around 8% at the top of the section.

Both illite and randomly interstratified clays are considerably more abundant than kaolinite in the clay interval, which is the reverse for much of the basal sand interval. As the clay becomes slightly sandier in the upper 3 m (in conjunction with a decrease in the amount of <2 μm material), the illite content relative to kaolinite progressively increases further from around 40% to 65% just beneath the carbonate blanket. The smectitic component of the interstratified clays in the interval is relatively constant at 20-30% apart from the base of the unit where it increases to around 50% (Supplement Table 3.1). Minor amounts of quartz occur in the <2 μm clay fractions. Dolomite and calcite occur in samples immediately below the carbonate blanket where there are isolated carbonate mottles in the clay interval.

Small variations in the width at half height of the 7Å XRD peak for kaolinite indicates little change in degree of order throughout the clay interval (Figure 4). On the other hand, illite is progressively more disordered up-section to the carbonate blanket.

3.1.2.2. Onkaparinga Trig

From about 6 m from the base of the Onkaparinga Trig section, massive red-green and grey-green clays with occasional blocky peds imparting a columnar appearance are in sharp contact with the underlying sand interval (Figure 5). A conspicuous green-grey clay horizon with large, white, soft calcareous mottles up to 30 cm occurs between

10-12 m above the base of the section: carbonate also impregnates the surrounding clay. The carbonate-mottled horizon can be traced intermittently northwards to the mouth of the Onkaparinga River. The top of the clay interval at ~14 m has a somewhat diffuse contact with a white sand with small ferruginous mottles marking the base of the overlying interval.

The clay interval has a relatively consistent particle size composition throughout and a relatively high silt content compared with the intervals above and below (Supplement Table 3.3). A mottled carbonate interval within the prominent clay unit does not register any obvious change in particle size composition.

Only kaolinite, illite and randomly interstratified clays were identified in the <2 μm fraction: the randomly interstratified clay includes some hydroxy interlayered smectite (Supplement Table 3.3). Below the mottled carbonate interval there is about 30% of kaolinite and interstratified clay with up to ~40% illite. At the base of the carbonate interval, illite increases markedly to around 50% while the concentration of kaolinite falls to between 15-25% and this persists to the top of the interval.

As indicated by the width of the 10 Å peak at half height, illite has a significantly lower degree of crystallinity than kaolinite compared with the basal sands and clays interval. The degree of disorder is a maximum in the base of the carbonate-mottled interval. These variations point to secondary alteration involved in the carbonate mottled and Fe-mottled intervals.

The composition of heavy mineral concentrates in >250 μm particle size fractions from two samples is given in Supplement Table 3.4. They have quite different assemblages of heavy minerals: a green clay with red ferruginous mottles from the lower part of the interval (RM312) is dominated by iron oxides with minor barite whilst a green clay from the upper part (RM323) contains abundant tourmaline and garnet with some ilmenite.

3.1.2.3. Hallett Cove

Massive vari-coloured (green-red to brown-green and green-grey) clays are at the bottom of the prominent clay interval here (Figure 6). The colour of the clays reflects yellow (goethitic - 10YR 6/8) and red (hematitic - 7.5R 3/4) colours of iron-mottling. Isolated sands, mottled and sometimes indurated, occur in the upper part of the interval, which is here directly overlain by the carbonate blanket. The uppermost sand interval is not recognised in this section.

Particle size data (Figure 6; Supplement Table 3.5) show that the clay interval has a consistent composition throughout with the clay content around 60% and the sand content usually less than about 20%. Illite is the major component of the clay fraction with less randomly interstratified material: kaolinite decreases in abundance relative to illite from the boundary with the basal sand interval.

From the point of view of crystallinity, there is no significant change in broadening of the (001) peak of kaolinite in contrast to that of illite which becomes systematically and significantly disordered (less crystalline) from the base to the top of the interval.

3.1.2.4. Snapper Point

A thick clay-rich sequence assigned to the prominent clay interval in the middle of the Plio-Pleistocene succession overlies the Hallett Cove Sandstone and Burnham

Limestone just above beach level (Figure 7). The surfaces of both the Burnham Limestone and the Hallett Cove Sandstone display distinctive karst and other weathering features that pre-date the deposition of the clay. Laminated sand intervals just above the Burnham Limestone occur at the base of a massive grey-green clay with rare blocky-prismatic structure and small yellow mottles which forms the dominant lithology of the clay interval. Its top is marked by sand-filled channels with planar bedding and iron-mottling forming the base of the overlying interval (Figure 8D). Of note is a distinctive carbonate-mottled horizon between 7-8.5 m above beach level (Figure 8E). This crops out intermittently in the same stratigraphic position for several kilometres to the north and varies in thickness from 1-2 m. Just north of Snapper Point, a sand-filled channel has eroded into the carbonate-mottled grey-green clay unit, indicating that the mottling pre-dates the erosional event.

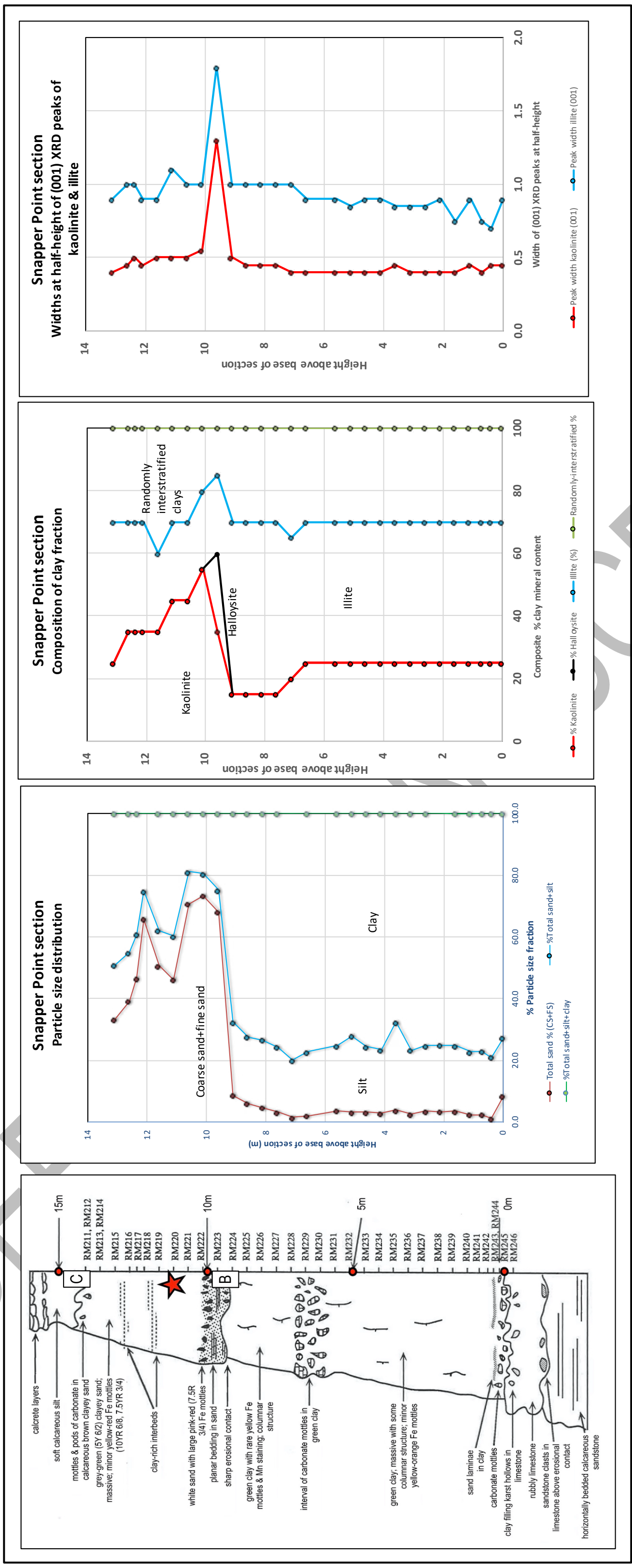

Figure 7. Annotated lithostratigraphy, particle size composition and mineralogy of the Plio-Pleistocene succession in the Snapper Point section, Willunga Basin. Red dots at right are 5 m intervals from the base of the succession set at 0 m; dashes indicate sample locations and numbers. All data tabulated in Supplement Table 3.6. B = top of the prominent clay interval; C = top of the uppermost sand interval. Red star = Fe mega-mottle sample.

In terms of particle size distribution, the clay interval contains mostly <2 μm material (more than ~75%) and silt (~20%) throughout. Illite dominates the clay fraction (~45%) with less abundant randomly interstratified material (~30%) and kaolinite (~25%) from the base of the interval to the carbonate mottled horizon (data tabulated in Supplement Table 3.6). The illite concentration increases relative to kaolinite in the green clay above the carbonate mottled interval. This matches a progressive influx of sand up-section from about 8 m and probably marks a change in depositional conditions or sediment source. There is very little change in the shapes of diffraction peaks through the clay interval but the illite peak is much broader than the kaolinite peak in all samples.

Non-clay minerals are minor components of the <2 μm particle size fractions and include quartz, feldspar, goethite and dolomite (Supplement Table 3.6). Quartz is present in all samples, and dolomite occurs in several samples from within the mottled carbonate horizon between 5 – 7 m above the base of the section. Goethite is present in all but one sample and links to the occurrence of small, yellow-orange iron mottles.

3.1.3. Upper sands and clays interval

The top of the prominent clay interval is marked in places by coarse sands filling channels eroded into it. These channel sand deposits are generally planar-bedded and gravels are rare. The channels have the form of broad troughs, up to 40 m across: smaller U-shaped channels occur higher in the sequence. The upper parts of the interval are usually interbedded clayey sands and clays with occasional sand interbeds and rare gravel layers. This interval is not recognised in the Maslin Bay (Figure 4) section. It was identified by Phillips (1988) in the Hallett Cove amphitheatre section (Figure 6) and elsewhere at the base of the carbonate mantle but not sampled in this study.

3.1.3.1. Onkaparinga Trig

At Onkaparinga Trig the base of the interval is a white, micaceous, sandy to silty horizon with small ferruginous mottles overlain by ~4 - 5 m of red-brown clays with several thin, sandy interbeds. In terms of particle size distribution (Figure 5), it is marked by a sharp influx of sand relative to silt and clay and is accompanied by a marked increase in kaolinite abundance relative to illite and randomly interstratified clay. Up-section the kaolinite content progressively decreases relative to the other clay minerals. Quartz is the main subsidiary mineral in the <2 μm clay fraction, with calcite and dolomite appearing with carbonate illuviation near the top of the interval (Supplement Table 3.3).

Excluding the Fe-mottled sand at the base of the interval, illite has a significantly lower degree of crystallinity than kaolinite and approaches that recorded in the middle part of the underlying prominent clay interval. By way of contrast, illite in the Fe-mottled base of the interval is as well-ordered as kaolinite.

Heavy mineral separates from two samples (Figure 5; Supplement Table 3.4) include abundant iron oxides, with subordinate, ilmenite, garnet and staurolite. Mica is co-dominant with iron oxides in one in contrast with tourmaline in the other.

3.1.3.2. Snapper Point

In this section the uppermost sand interval consists of isolated sand-filled channels with planar bedding and iron-mottling overlain by massive grey-green, Fe-mottled clayey sands with thin clay interbeds (Figure 7). In terms of particle size distribution, there is a clear distinction between it and the underlying prominent clay interval in the sense that it is dominated by sand and clay with only minor silt. Relative to sand, the abundance of clay-sized material increases up-section.

The basal sand unit in the interval has a high kaolinite content (up to ~50%) relative to illite and interstratified clays, but this decreases up-section where illite becomes dominant (Supplement Table 3.6). Of particular note is the occurrence of halloysite (both 7 Å and 10 Å forms) in one sample from this horizon, matching a decrease in randomly interstratified clay content.

Measurements of peak widths at half height of kaolinite and illite show a significant decrease in crystallinity (increase in peak broadening) in the halloysitic sample, pointing to some form of secondary alteration in association with Fe-mottling. Otherwise, there is very little change in the shapes of diffraction peaks throughout the whole section, although illite is consistently less well ordered than kaolinite.

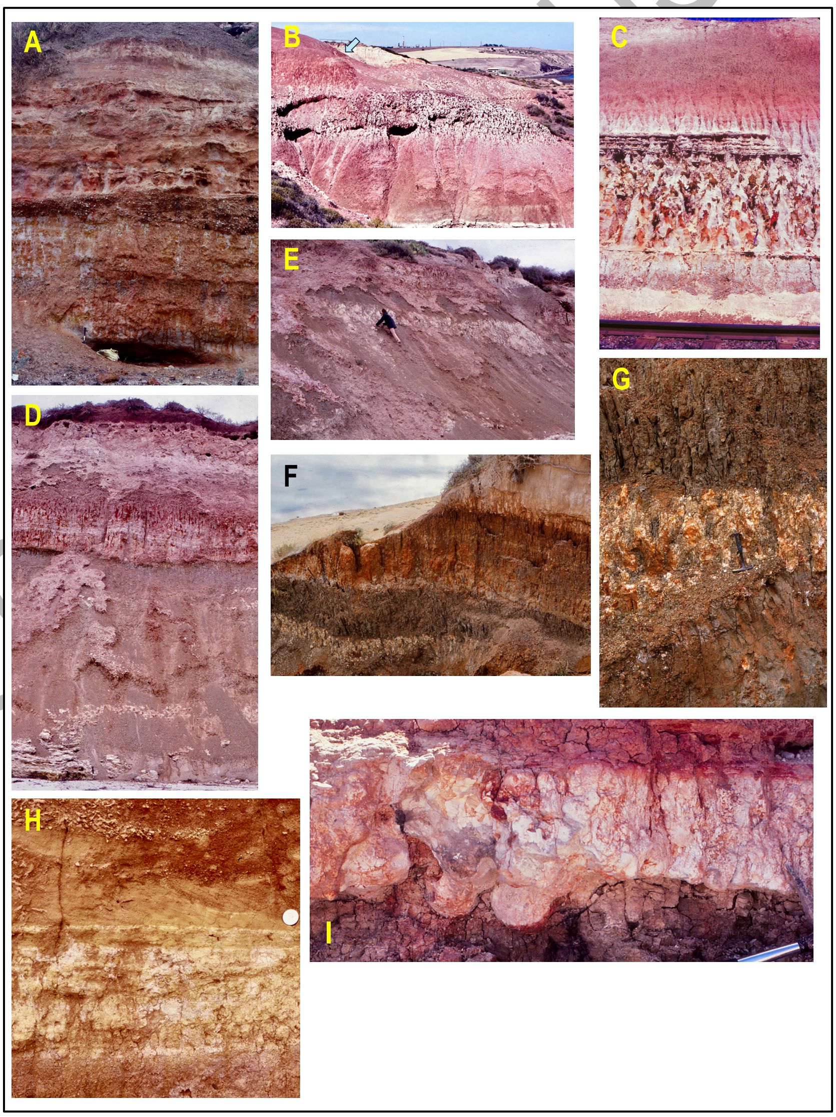

Figure 8. Field photographs. (A) Basal Plio-Pleistocene interval of sands, clays, grits and gravels south of Robinson Point showing upward fining units at the bottom of the section topped by cross-bedded gravels filling a broad channel in sandy clays. Dark coloured grey-green clays of the overlying prominent clay interval top the section. (B) Amphitheatre section at Hallett Cove showing Fe mega-mottled zone (~2.5 m thick) in yellow to red sandy clays and sands of the basal Plio-Pleistocene sequence. This unconformably overlies white Hallett Cove Sandstone and is overlain (from arrow) by reddish clays of the prominent clay interval. (C) Distinctive Fe mega-mottled horizon in basal Plio-Pleistocene sands filling a channel eroded into Neoproterozoic bedrock in a railway cutting south of O'Sullivan Beach Road. Thinly-bedded and indurated sands above are overlain by reddish clays (bleached at the base) of the prominent clay interval in the study area. At right, the clay interval fills a secondary erosional channel cut in the basal sediments. (D) Sands of the uppermost sand and clay interval (with hematite mega-mottles as vertical 'stringers') filling an erosional channel in the underlying prominent clay interval just north of Snapper Point. Late Pliocene Burnham Limestone and underlying Hallett Cove Sandstone crop out at the base of the section. Carbonate silt-calcrete blanket at the top of the section. (E) White carbonate-mottled interval within grey-green clays of the prominent clay interval, Snapper Point. Unstable, active slopes are a consequence of the ubiquitous self-mulching character of these clays. (F) Erosion gully at mouth of Onkaparinga River showing the prominent clay interval (dark brown) at the base of the section with a 1 m thick interval of mottled carbonate. Overlying reddish sediments assigned to the uppermost sand and clay interval are capped by a thick calcareous silt and calcrete blanket. Section is approximately 7 m thick. Note the conspicuous prismatic shrink-swell pedal structure in the brown clays and more distinctive columnar structures in the red clayey sands above. (G) Details of carbonate horizon in the brown clay interval at the Onkaparinga River mouth site showing pervasive prismatic shrink-swell structure in the underlying and overlying clays. Goethitic Fe-mottles occur in both the carbonate horizon and the clays. Fissures and 'pockets' in the carbonate horizon are generally clay-filled. Hammer about 30 cm long. (H) Lower sand section in the basal Plio-Pleistocene interval at Onkaparinga Trig with pinkish halloysitic horizon at the bottom, cream-white alunitic alteration above, and an overlying interval of cross-bedded sands and angular gravels. 3 cm diameter coin for scale. (I) Thick seam of white alunite, generally conformable with bedding, in the base of the Plio-Pleistocene sequence (lowermost sand-clay-grit-gravel interval) between Port Noarlunga and Witton Bluff. The upper and lower boundaries of the alunite seam are sharp; the lower boundary presenting as a series of bulbous masses protruding down into the underlying sediments and the upper boundary as the convex tops of vertical columns projecting upwards. Part of hammer handle at bottom right for scale.

3.2. Synthesis of lithostratigraphic data and facies distribution

A synthesis of all lithostratigraphic data for the intervals in the four key sections (detailed above) and eight subsidiary sections (data assembled in Supplement Section 2) provides a basis for describing the distribution of facies in a north-south section through the Embayments (Figure 9).

3.2.1. Basal sands, clays, grits and gravels

The oldest part of the succession, an interbedded sequence of clays, sandy clays, sands, grits and gravels 5 - 10 m thick, overlies erosional surfaces on Neoproterozoic bedrock, Permian glacigenes or Oligo-Miocene and Pliocene marine limestones. The basal sediments and those near the top of the interval are dominantly sands and sandy clays with rare thin gravel beds: discontinuous gravel lenses are common in central parts of the interval. Clasts are mostly angular to sub-rounded quartz, quartzite, siltstone and ferricrete which vary in size from a few mm to 10 cm. In places, coarse gravels occur at the base of the interval (Figure 8A). Sand and gravel intervals are both planar- and cross-bedded, the latter being more common in basal parts of the interval. In contrast to the coarser intervals, interbedded sandy clays have no discernible bedding.

In some sections near the base of the interval there are upwards-fining cycles (up to 1 m-thick) of poorly-sorted, angular to sub-rounded gravels passing upwards into silt and clay beds. The finer units commonly have a secondary blocky, prismatic structure which masks primary sedimentary features. Bioturbation has the form of 2 – 10 mm diameter, vertically-oriented, cylindrical tubes, some of which are filled with clay.

Significant secondary alteration in the form of thin seams and isolated rounded masses of white alunite in the basal sands are generally associated with halloysite-impregnated nodular masses. The alunite occurs in intervals up to 2 m thick with an unusual pink-red colour. Prominent Fe mega-mottling characterises bleached and somewhat indurated sands in central parts of the interval. Preferential bleaching along fractures and cracks accounts for a coarse rectangular pattern of iron-mottling. Smaller, less prominent yellow-orange ferruginous mottles occur in associated clayey intervals.

The interval is well exposed in the Noarlunga Embayment and the northern part of the Willunga Embayment and is also well developed immediately adjacent to the fault scarp at the southern extremity of the Willunga Embayment (Figure 9). In places, for example at Sellicks Beach, Maslin Bay, Witton Bluff and Hallett Cove, the basal sands and gravels are interbedded with the Late Pliocene marginal marine Burnham Limestone. In the northern part of the Willunga Embayment, the interval unconformably overlies Neoproterozoic sedimentary rocks and a ferruginised conglomerate near Ochre Point considered by earlier workers to be the Hallett Cove Sandstone (Glaessner & Wade, 1958; Ward, 1966; Stuart, 1969). Between Witton Bluff and the Onkaparinga River mouth in the Noarlunga Embayment, coarse gravels occur at the base of the interval. Coarser gravels are found in the thickest section of the interval adjacent to the Willunga Fault Escarpment at Sellicks Beach.

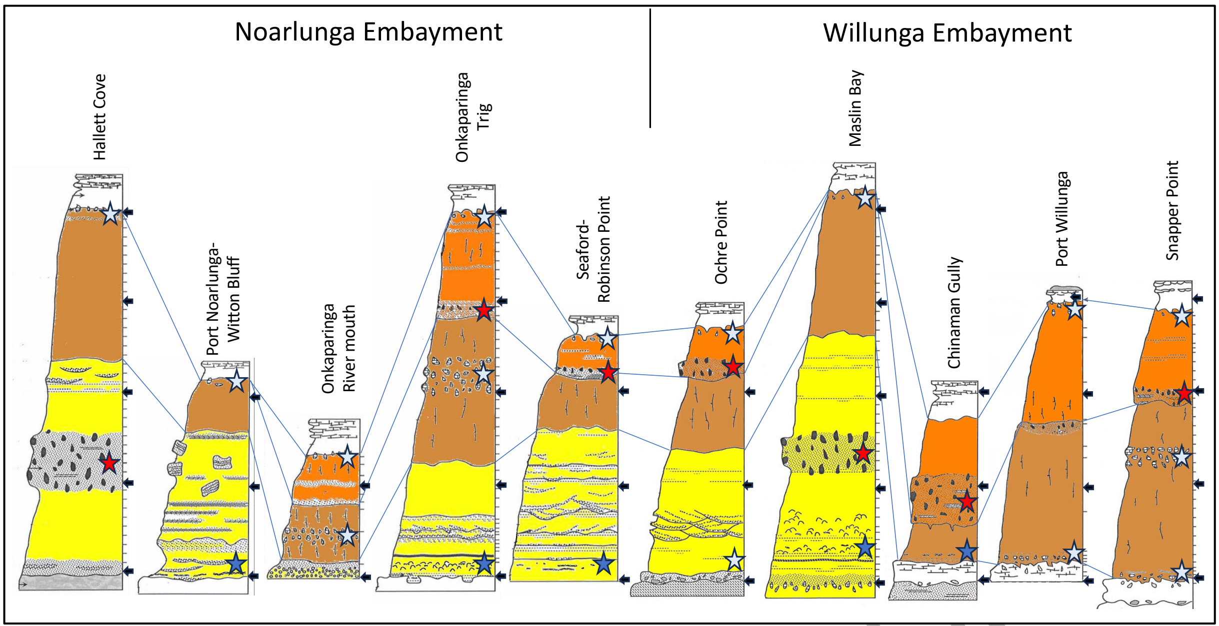

Figure 9. Overview of facies development in Plio-Pleistocene non-marine succession in coastal cliffs in the Noarlunga and Willunga Embayments (Figure 1 for locations). Details of stippling as in annotated sections in Figures 4-7. Depositional sequence marked by the basal interval of sands, clays, grits and gravels (yellow); prominent clay interval (brown); upper sands and clays (orange); and carbonate blanket with calcretes (white). Neoproterozoic bedrock or Permian glacigenes (grey stippled) and Cenozoic limestones (white) at the base of sections. Post-sedimentary alterations include carbonate mottled intervals (pale blue stars); bleached and Fe mega-mottled zones (red stars); alunite-halloysite intervals (dark blue stars). Black arrows at right are 5 m intervals from the base of the succession at 0 m: dashes in key sections are sample locations.

3.2.2. Prominent clay

The middle interval in the succession is dominantly clay with a self-mulching surface which effectively obscures any primary sedimentary structures. Typical sections feature a massive, red to grey-green clay with rare thin (~1 mm) laminae of fine sand near the base. Rounded, sand-sized quartz grains are visible. The contact between the clay and the underlying sand interval is everywhere sharp.

Apart from a conspicuous self-mulching surface character, coarse blocky peds with slickensides and manganese oxide coatings are common in exposures (Figure 8G). Small orange-yellow ferruginous mottles are also present, while red ferruginous mottles tend to occur in central and upper parts. There are some discontinuous intervals of carbonate mottles up to 2 m thick in the upper half of the unit in several sections (Figures 8D, F and 9) and these mimic remnant subsoil horizons in soils (usually designated B$_{Ca}$).

In contrast to the basal interval of sands, clays, grits and gravels, the conspicuous prominent clay interval in coastal cliffs is exposed almost continuously between Hallett Cove and Sellicks Beach: the thickest sections (up to 14 m) occur near Snapper Point and Onkaparinga Trig. In central parts of the Willunga Embayment the basal sand interval is absent and the clay unconformably overlies Burnham Limestone: in some sections there are carbonate mottles within the basal horizons.

3.2.3. Upper sands and clays

These channel sand deposits are generally planar-bedded and gravels are rare. The channels have the form of broad troughs, up to 40 m across, and smaller U-shaped channels. The upper parts of this interval are usually interbedded clayey sands and clays with occasional sand interbeds and rare gravel layers. The latter contain pebble-sized, sub-rounded clasts of quartzite and siltstone. In some sections these sands have the form of poorly defined sheets rather than isolated channels but tend to be devoid of bedding structures. The sand sheets are upward-fining and commonly interbedded with finer sandy clay units. Secondary alteration usually takes the form of iron mottling and bleaching: some induration of mottled sands is common. The uppermost contact of this interval with the overlying carbonate blanket tends to be gradational over ~1 m or so and is complicated by illuviated vertical mottles and bands of carbonate.

The upper sand and clay interval is widely distributed throughout the Embayments but not recognised in the Hallett Cove, Port-Noarlunga-Witton Bluff and Maslin Bay sections. Its base is commonly marked by coarse sands filling channels eroded into the underlying clay interval. Many contain conspicuous Fe mottling (Figure 8D).

3.3. Comments on environments of deposition

Sediments at the base of the non-marine succession interfinger with the Late Pliocene marginal marine Burnham Limestone, indicating an estuarine environment of deposition. Thin beds with dolomite in some sections suggest an interaction between Mg-containing groundwaters and saline or marine waters (e.g., von der Borch & Lock, 1979).

The overlying sediments present as a sequence of gravels, sands, silts and clays with sands and sandy clays predominating. Horizontal, planar bedding characterises some sands whilst planar cross-bedding is common in grits and gravels. Gravels tend to fill broad channels eroded into underlying units but also occur as tabular bodies that can be traced for several hundred metres. Upward fining sequences from gravel to sand, silt and clay are observed and many show forms of pedogenic modifications in the finer sediments, indicating periods of stasis. Thus, sediments with both bed-load and suspended-load characteristics are recognised. There is no evidence of organic remains. In a general sense, a distributive fluvial environment (Plink-Björklund, 2021) with streams and channels meandering across alluvial plains is implicated (Ventra & Clarke, 2018). Ward (1966) ascribed these sediments to fluviatile and alluvial environments; Stuart (1969) suggested they were essentially fluvial in origin; and McGowran et al. (2016) proffered an alluvial fan environment.

The middle interval in the succession is a massive, grey-green clay with rare fine sandy interbeds: the upper interval consists of interbedded sands and clays. The latter includes planar-bedded sands with rare gravel horizons occupying broad channels cut into the underlying clays: these grade upwards into interbedded sequences of sands and clays. In places there are laterally extensive tabular sand bodies.

Our working hypothesis is that the massive clays in the middle interval are suspended load sediments deposited in overbank or lacustrine environments in more distal parts of an alluvial plain environment, as understood in distributive fluvial systems (Plink-Björklund, 2021). The overlying lens-shaped and tabular sand bodies probably represent minor stream channels and crevasse splays. Bioturbation indicates hiatuses in deposition, subtle ferruginous mottling patterns point to redoximorphic conditions, and prismatic to blocky pedal structures reflect shrink-swell processes due to wetting and drying. Carbonate mottles in clays in the upper parts of the interval are likely to be remnants of B_{Ca} horizons of soil profiles formed in aeolian calcareous silts deposited intermittently over the alluvial landscape (Phillips & Milnes, 1988) and may herald the formation of the thick blanket of calcareous material overlying the regional landscape. The latter marks a significant change in sediment source and depositional environment accompanied by a drier climate.

Clay minerals in the sediments are dominantly kaolinite, illite and randomly interstratified illite-smectite most likely sourced from elevated soil landscapes to the east on Fleurieu Peninsula (Figure 1). The basal interval and sandier intervals above contain more kaolinite than illite or randomly interstratified clay while finer sediments, particularly those in the prominent clay interval, contain higher proportions of illite and randomly interstratified clay. Although rare in the study area, smectite is abundant in fine-grained sediments in parts of the basal interval where the concentration of randomly-interstratified clay is absent or low. It may have formed by alteration of randomly interstratified illite-smectite and illite in a sedimentary environment with poor drainage (McArthur & Bettenay, 1974; Meyer & Pena Dos Reis, 1985; Sheard & Bowman, 1994).

The assemblages of heavy minerals are broadly similar throughout the three intervals (Table 1; Supplement Tables 3.2, 3.4) and don't offer any indication of a change in provenance.

4. Stratigraphic scheme

Various schemes have been proposed for the stratigraphic subdivision of the Plio-Pleistocene succession in the Willunga and Noarlunga Embayments. Some authors used a combination of sedimentary and secondary alteration features to identify and distinguish specific intervals; others made tentative correlations with known units in other locations based on general lithological features. For example, Ward (1966) divided the basal sequence of gravels, sands, silts and clays into two, with Ochre Cove Formation (a unit of 'alluvial' sands with lenses of grit and gravel) unconformably overlying Seaford Formation ('fluviatile' sandy clays and clays interbedded with pebble beds, gravels and grits). Daily et al. (1976) referred most of the sequence above the Pliocene Hallett Cove Sandstone (including Ward's Seaford and Ochre Cove Formations) to the Hindmarsh Clay but, like Forbes (1983), separated out an uppermost clay unit as Keswick Clay, both of which were initially named in the Adelaide Plains Sub-basin (Firman, 1966). Ward included the carbonate blanket and its cemented calcretes at the top of the succession in his Ngaltinga Clay, and this appears to have been a basis for assigning it an aeolian origin. This was not accepted by Daily et al. (1976) and Forbes (1983) who identified the carbonate blanket with an upper member of the aeolian Bridgewater Formation and a calcrete caprock separately, as Bakara Calcrete of pedogenic origin. Phillips (1988) and Phillips & Milnes (1988) included these two units in their unnamed carbonate 'blanket' (named by Sheard & Bowman [1987a, b; 1994] in the Adelaide region as the '*Carbonate Pedoderm*'). More recent work extending inland from the coastal cliff exposures in the embayments used Ward's stratigraphic scheme or modifications of it (Preiss, 2019a; Aldam et al., 2022, Bourman et al., 2022).

Our suggested stratigraphic scheme is summarised in Figure 10 alongside others. It was initially described by May (1992): it focusses on the sedimentological features observed in the coastal cliff sections in conjunction with mineralogical and other analyses and ignores secondary alteration features. A fundamental issue is that the Seaford and Ochre Cove Formations in Ward (1966) couldn't be consistently distinguished in the coastal sections from a lithological aspect, given that the Seaford Formation was identified by Ward (1966) as '*sandy clays and clays and variously consolidated sands interbedded with pebble beds, gravel beds, and grits*', and the Ochre Cove Formation as '*thick horizontal alluvial sandstones (sand rock) and clayey sands with lenses of grit and angular gravel, and poorly sorted gravel beds of varying thickness with heavy conglomerates'*. Such sedimentary facies are laterally and vertically variable in the cliff sections, as might be expected in a fluvial-alluvial landscape. However, they are quite distinct from the overlying dominantly clay interval.

Secondly, Ward (1966) included yellow-grey weathering colouration, 'limonitic' bands and the presence in many places of red, pink, and occasionally purple colours together with alunite 'interbedded' with clays in the Seaford Formation. Descriptions of the 'Ochre Cove Formation' included its variegated yellow-red-grey weathering colouration, conspicuous coarse red and reticulated ferruginous mottling, and cavernous-weathering (Ward, 1966). These characteristics are secondary alterations related to groundwater environments and are not useful in identifying and distinguishing sedimentary formations. Also, our detailed lithological observations and mineralogical-granulometric data for the sequences do not show support any subdivision of the basal clastic interval into two parts. As well, the unconformity surface identified by Ward (1966) at the top of the Seaford Formation in his Type Section is not unique: many of the coarse sand and gravel units higher or lower in the stratigraphy fill erosion channels or hollows eroded into the underlying sediments. Accordingly, we suggest that the basal interval of gravels, sands, silts and clays is best mapped as a single entity encompassing Ward (1966) Seaford and Ochre Cove formations, and named the Robinson Point Formation with the Type Section at Onkaparinga Trig (Figures 5 and 9).

The overlying prominent clay is assigned to the basal part of the Ngaltinga Formation (Neva Clay Member) which corresponds to the basal part of Ward's Ngaltinga Clay, and the upper formation of sands and clays which Ward (1966) and others did not recognise, the Snapper Point Sand Member (Phillips & Milnes, 1988; May, 1992; Figure 10). The Type Section for the Ngaltinga Formation is at Snapper Point (Figures 7 and 9). As defined by Phillips & Milnes (1988), the overlying carbonate 'blanket' is separated from the Ngaltinga Formation.

Figure 9 shows that the lithostratigraphic units are laterally variable but that the thickness of the succession, overall, is similar. This includes the Hallett Cove section, which is somewhat isolated to the north in a Permian glacial depression in bedrock within the Eden Fault block, and the Ochre Point section which overlies bedrock uplifted by the Ochre Cove-Clarendon Fault (Figure 3). A very thick section at Sellicks Beach in the scarp foot of the Willunga Fault is an exception (May, 1992).

<table>
<tr><th>Ward (1966)</th><th colspan="2">Firman in Daily et al. (1976)*</th><th>Forbes (1983)</th><th>Bourman et al. (2022)</th><th colspan="2">Phillips (1988), Phillips & Milnes (1988), May (1992), this paper</th></tr>
<tr><td>Waldeila Formation</td><td colspan="2"></td><td></td><td>Waldeila Formation</td><td colspan="2" rowspan="7"></td></tr>
<tr><td>Ngankipari Sand</td><td colspan="2">Light brown silty fine sand</td><td>Semaphore Sand</td><td>Nangkipari Sand</td></tr>
<tr><td rowspan="2"></td><td colspan="2" rowspan="5"></td><td rowspan="2">Alluvium of river terraces & flood plains (Waldeila Formation in part)</td><td>Unnamed alluvium</td></tr>
<tr><td>Unnamed alluvium</td></tr>
<tr><td rowspan="2">Christies Beach Formation</td><td>Surficial materials & soils of slopes & plains (Callabonna Clay, Pooraka Formation, Christies Beach Formation)</td><td>Pooraka Formation</td></tr>
<tr><td rowspan="2"></td><td>Kurrajong Formation</td></tr>
<tr><td>Taringa Formation</td><td>Taringa Formation</td></tr>
<tr><td rowspan="4">Ngaltinga Clay - thick, non-marine, partly calcareous, grey to olive-grey clays & sandy clays with lenses of clayey sand & white marl. Red & yellow staining masks grey colour. Thin gravel lenses Discontinuous calcareous bands. Grades upards into marls with hard, dense, banded kunkar horizon near land-surface. Considered to be aeilian.</td><td colspan="2">Baraka Calcrete</td><td>Bakara Calcrete</td><td rowspan="4">Ngaltinga Formation</td><td colspan="2" rowspan="2">Carbonate 'blanket' ('Carbonate Pedoderm')</td></tr>
<tr><td colspan="2">Upper member Bridgewater Formation</td><td>Bridgewater Formation (partly aeolian gravelly carbonate silt - upper member); sand Ngankipari Sand</td></tr>
<tr><td rowspan="6">Hindmarsh Clay</td><td rowspan="2">?Keswick Clay</td><td rowspan="2">Keswick Clay - brown & green-grey clay (?Taringa Formation)</td><td>Sands & clays with rare gravels (Snapper Point Sand Member)</td><td rowspan="2">Ngaltinga Formation</td></tr>
<tr><td>Thick grey-green clay (Neva Clay Member)</td></tr>
<tr><td>Kurrajong Formation**</td><td>Light greyish brown clay with red mottles</td><td rowspan="3">Hindmarsh Clay (brown, red, olive clay, sandy clay, sand, gravel lenses). Ngaltinga Clay (in part). Includes lower sand unit possibly equivalent to: Carisbrooke Sand, Ochre Cove Formation, Seaford Formation</td><td rowspan="2">Ochre Cove Formation</td><td colspan="2" rowspan="3">Sands, clays, grits and gravels (Robinson Point Formation)</td></tr>
<tr><td>Ochre Cove Fomation - alluvial sandrock & clayey sands, lenses of grit & angular gravels; conglomerates. Variegated colours. Coarse, red reticulated iron-mottled sandstones, cavernous weathering.</td><td>'Ardrossan Soil'</td></tr>
<tr><td rowspan="2">Seaford Formation - fluviatile sandy clays & clays, variously consolidated sands with pebble beds, gravel beds & grits</td><td rowspan="2">Red mottled sandy clay with olive clay at base</td><td>Seaford Formation</td></tr>
<tr><td>Burnham Limestone</td><td>Burnham Limestone</td><td colspan="2">Burnham Limestone</td></tr>
<tr><td>Hallett Cove Sandstone</td><td colspan="2">Hallett Cove Sandstone</td><td>Hallett Cove Sandstone</td><td>Hallett Cove Sandstone</td><td colspan="2">Hallett Cove Sandstone</td></tr>
</table>

Figure 10. Schemes for subdivision of the Late Cenozoic succession in coastal cliffs in the Willunga and Noarlunga Embayments. *Hallett Cove amphitheatre. **Restricted to scarp-foot zones along faults. Column at at right is the scheme adopted in this paper.

5. Unravelling physical and chemical overprints in the succession

5.1. Forms of overprinting

In terms of superficial alteration, the sands and clays in the cliff sections are pervasively reddened and yellowed by secondary iron oxides. To some extent this is a consequence of weathering on exposure. Other distinctive features include blocky-columnar structures in sandy clays and the self-mulching character of the Neva Clay Member of the Ngaltinga Formation. These features tend to mask primary sedimentary structures and are also probably accentuated by exposure.

Less obvious forms of alteration include bioturbation, which points to still-stands in sedimentation and probable surface exposure in fluvial/alluvial environments, and relatively subtle hematite and goethite mottling which tends to impart specific colours to the sediments but does not generally mask their primary sedimentary features. These sediments retain their primary clay mineralogy. In this category, carbonate (calcite, dolomite) mottling in particular horizons in parts of the succession is an indicator of sedimentary or pedogenic origins.

Conspicuous, locally intense and pervasive forms of post-depositional alteration include bleached and Fe mega-mottled sand horizons and distinctive zones of alunite and halloysite formation, both of which mask most primary sedimentary features. The composition of the clays and associated minerals in these intervals differs significantly from that in the unaltered surrounding sediments and provides clues to the types of reactions responsible for the alteration.

5.1.1. Syn-depositional overprints

5.1.1.1. Bioturbation

Abundant small, circular, vertical or sub-vertical tubes 0.5-2 mm in diameter occur in grey silty-clays in basal parts of the Robinson Point Formation in the Onkaparinga Trig section. The walls of many of these structures have very thin red-brown coatings of clay different from that in the encompassing sediment. There are also larger tubes with diameters between 5-10 mm filled with red-brown clay. None of them are longer than about 5 cm and branching structures were not observed. Similar features occur in the middle parts of the Robinson Point Formation, for example to the north of Witton Bluff and south of Moana. Just south of Blanche Point, vertical tubular structures up to 1 cm in diameter filled with laminae of illuviated clay occur within sandy sediments at the boundary between the Robinson Point and Ngaltinga Formations, and in the basal part of the Snapper Point Sand. All are in intervals that are similar in appearance to the A_2 horizons of some soil profiles and may reflect the burrowing activities of insects or worms, indicating breaks in deposition sufficient to support biological activity and, in some cases, long enough to promote soil formation (Retallack, 1988).

5.1.1.2. Shrink-swell structures

A coarse blocky prismatic structure is common in clays (Figure 8F), for example in the Ngaltinga Formation in sections at Onkaparinga Trig (Figure 5) and Snapper Point (Figure 7). This resembles pedality in clay subsoil horizons due to wetting and drying, and is a likely consequence of the abundance of randomly interstratified clays. In some cases, the ped surfaces have slickensides (indicative of differential sliding of adjacent blocks during shrink-swell movement) and Mn oxide coatings (precipitated from infiltrating water). In addition, the surface self-mulching character and consequent erodibility of clays in the Ngaltinga Formation accounts for a general rounded nature of their exposures in the coastal cliffs (Figure 2). Primary sedimentary structures, including bedding, are poorly preserved in these intervals.

5.1.1.3. Carbonate-mottling

Isolated masses of dolomite in the metre or so of sediments overlying the Burnham Limestone at several locations in the Willunga Embayment form discontinuous horizons that can be traced laterally for tens of metres. The dolomite masses, up to 20 cm in size, have sharp boundaries and contain thin fractures filled with clays or sands from the surrounding sediment, suggesting exposure and drying prior to a resurgence of sedimentation. In contrast to samples of the Burnham Limestone itself, they contain only small amounts of calcite (data tabulated in Supplement Table 5.1). It is likely that these are altered Burnham Limestone equivalent formed near shorelines in a marginal marine environment.

By way of contrast, carbonate-mottled horizons of variable thickness and lateral extent in the Neva Clay at several localities along the coast resemble the remnant B_{Ca} horizons of some soils. In the Willunga Embayment at Snapper Point (Figures 7 and 8E), one such horizon up to 1.5 m thick contains irregularly-shaped masses of carbonate that are usually soft and friable. The carbonate tends to have a vertical, blocky-prismatic form similar to that developed in the surrounding clays. Individual carbonate masses are separated by up to 15 cm of clay and fine sand and have sharp borders that are commonly smoothed and slickensided. Rare thin tubes, several mm in diameter, and possible rhizoliths occur in some. The carbonate horizon is intermittently exposed laterally for at least 400 m and generally has a relatively sharp upper contact with overlying clays. Its base is somewhat diffuse with small, isolated carbonate masses occurring up to 30 cm below the main horizon.

In the Noarlunga Embayment, a discontinuous band of carbonate masses up to 2 m thick in the Onkaparinga Trig section (Figure 5) can be traced laterally, albeit intermittently, for up to 50 m. The masses are very similar to those at Snapper Point and contain small hollows and fractures filled with clay. The carbonate horizon exposed in a vertical section at the mouth of the Onkaparinga River (Figure 8F, G) is around 1 m thick: it has a strong vertical structure and sharp upper contact with the overlying sediment. The base of the horizon is somewhat irregular with isolated carbonate masses extending down into the underlying clays. About 100 m south of Witton Bluff, a mottled carbonate horizon of variable thickness up to 1 m is exposed in the cliff face at the boundary between the Robinson Point and Ngaltinga Formations.

In the Onkaparinga Trig and Snapper Point sections, the clay fraction of the mottled carbonate horizons is dominated by illite with lesser amounts of kaolinite and randomly interstratified clay (Figures 5 and 7). Differences in the proportions of kaolinite and illite in <2 µm fractions in the carbonate from those in underlying sediments imply a change in environmental conditions. The carbonate masses themselves are mainly dolomite with subordinate calcite. There is a systematic change in carbonate mineralogy from the base to the top (Supplement Figure 5.1): mottles in the lower part of the horizon are exclusively dolomite whereas calcite is dominant in the uppermost parts. The marked enrichment in dolomite relative to calcite with depth mimics that in many calcrete profiles in southern South Australia (Milnes, 1992).

5.1.1.4. Fe-mottling

Subtle iron-mottling in most sections is a consequence of Fe mobilisation and precipitation in a fluctuating moisture regime, for example periodically wet sediment or subsoil environments (Schwertmann & Taylor, 1989). Here, hydromorphic conditions are such that hematite and goethite can precipitate from Fe-bearing groundwaters in oxidic sites associated with cracks, fractures and bioturbation, as noted by Sheard & Bowman (1987a, 1994) and Sheard et al. (2015).

5.1.2. Post-depositional overprints

5.1.2.1. Iron mega-mottling

Prominent lenses and horizons with red Fe mega-mottles in bleached and somewhat indurated coarse sands are a striking feature of the succession (Figure 9). They are also conspicuous in the Plio-Pleistocene sequences in cliffs on Yorke Peninsula and Kangaroo Island on the western and southern coasts of the St Vincent Gulf.

At Hallett Cove, the prominent Fe-mottled interval in the central part of the Robinson Point Formation (Figure 6) is a bleached, indurated sand with rare stone lines and planar bedding. The mottles are large, red, indurated, up to 50 x 20 cm in size and tend to have a vertical orientation: some have a yellow-orange cortex. In a channel eroded into underlying Precambrian bedrock in a railway cutting adjacent to O'Sullivan Beach Road (Figure 8C) there are flat-bedded, somewhat bleached and indurated white-grey sands of the Robinson Point Formation with Fe mega-mottles (red, hematitic with yellow cortices) near the base of the channel. At Onkaparinga Trig (Figure 5), large hematitic mottles are confined to a sand interval at the base of the Snapper Point Sand. The mottles are less indurated and smaller (up to 30 cm) than those at Hallett Cove: golden yellow cortices of jarosite occur in some. There are similar intervals in the sections at Snapper Point (Figures 7 and 8D), Chinaman Gully and Ochre Point (Supplement Figures 2.3, 2.5). Large (up to 40 cm) vertically-oriented hematite mottles with yellow cortices are common in a 2 m thick, bleached white sand that is strongly indurated and stands out in coastal cliffs as a resistant bench in the central part of the Robinson Point Formation at Maslin Bay (Figure 4).

Chemical analyses of Fe mega-mottles associated bleached sediments and some unaltered sediments are graphed in Figure 11 (data tabulated in Supplement Table 5.2). In terms of chemical composition, both Fe mottles and sediments contain more than ~60% SiO_2 (due to a preponderance of quartz sand and silt) and less than ~25% Al_2O_3 (mostly in clay minerals), in contrast to the composition of <2 µm particle size fractions in which clay minerals are dominant (Figure 11A). The iron content (measured as Fe_2O_3) is somewhat higher in the separated clay fractions (averaging around 10%) than in the bulk sediments (around 5%) in which it is diluted by SiO_2 from the abundant quartz. Figure 11B shows that, relative to unaltered bulk sediments and separated clay fractions, Fe-enrichment in mottles is matched by a decrease in total alkalis (K, Mg, Ca) and Al in bleached sediments.

Colour variations in mottles from dark red and red-brown through to yellow-brown reflect differences in iron oxide mineralogy: the ratios of the heights of the main goethite (110) and hematite (110) XRD peaks provide a crude measure of the relative proportions of these two minerals (Table 2). Jarosite is a distinctive golden-yellow alteration product of hematite of some mega-mottles. The widths at half-height of (110) XRD peaks for hematite and goethite indicate differing degrees of crystallinity but are similar for each mineral in the same sample. Based on the positions of goethite (110) and (111) peaks there is little (2-6 mole%) Al substitution in the goethite. Some bulk sediment samples and the <2 µm fractions separated from them display a broad region of high background centred on ~4.1 Å in XRD traces indicating poorly crystalline opaline silica.

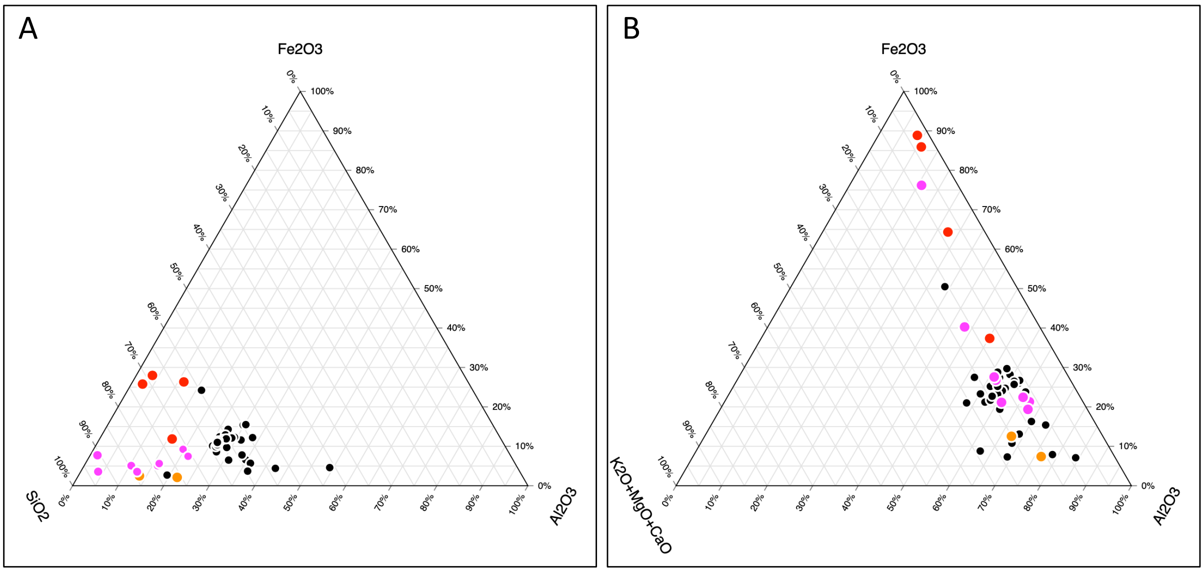

Figure 11. Graphs of chemical compositions of Fe mega-mottles (red circles), associated bleached sediments (orange circles), bulk sediments (pink circles), <2micron particle size separates from sediments (black circles). Data tabulated in Supplement Table 5.2.

Table 2. Mineralogical compositions of selected Fe mega-mottles. K=kaolinite; M=mica; Q=quartz; F=feldspar; H=halite. nd=not detected. *at half height

Sample number	Location	Sample description	Formation	Dominant iron mineral	Goethlte (110) peak (Å)	Peak width (2θ)*	Goethlte (111) peak (Å)	Al substitution	Hematlte (110) peak width (2θ)*	%Fe_20_3 (XRF)	Ratio goethlte (110) to hematite (110)	Munsell colour	Other minerals (XRD)
RM28-1	Sellicks Beach, upper part of cliffs along access path. 0.6 km south of boat ramp	3.5 m below cliff-top. White-grey gravelly and sandy clay from within iron mottled interval	Robinson Point Formation							2.18			M,K,Q,F
RM28-2	Sellicks Beach, upper part of cliffs along access path. 0.6 km south of boat ramp	3.5 m below cliff-top. Hard red sandy-clay mottle	Robinson Point Formation	goethite = hematite	4.177	0.5	nd	None	0.3	22.79	1.04	10R4/6	M,K,F,Q
RM40	Ochre Point	Hard red mottle within white sandy lens	Snapper Point Sand Member	goethite = hematite	4.18	0.6	2.448	None	0.4	25.42	1.73	10R3/6	K,M,Q,F
RM41	Ochre Point	Soft red mottle immediately above RM40	Snapper Point Sand Member	goethite = hematite	4.167	0.5	2.446	2-6 mole%	0.4	27.37	1.59	10R4/6	K,M,Q,F
RM264	Maslin Bay. 6.5 m above Burnham Ls	Large, indurated red sandy mottle adjacent to RM263.	Robinson Point Formation	hematite	4.185	0.6	nd	None	0.7		0.83	10R6/3	K,M,Q,F,H

Fe mega-mottled intervals reflect quite aggressive alteration resulting in bleached zones (from which Fe and other cations have been leached and exported) and large hematite-rich patches in which Fe oxides remain or have accumulated. Both the Fe mottles and the bleached zones are somewhat indurated due in part to precipitation of silica from solutions permeating the sediment matrix. This points to an environment in which acid and somewhat reduced groundwaters moved downgradient along flowpaths in pervious horizons facilitating dissolution and leaching, principally of clay minerals, whereas in adjacent less permeable zones, localised oxidic conditions sustained or precipitated hematite and goethite. Pale yellow jarosite fills fissures and pores in the cortices of some hematite mega-mottles and is the product of a later phase of acid-sulphate alteration of hematite and clay minerals.

Palaeomagnetic analyses of iron-mottles in two sections through the succession at Sellicks Beach and Hallett Cove were reported by Pillans & Bourman (1996, 2001). At Sellicks Beach, Fe mega-mottles near the top of the Robinson Point Formation, ~25 m above the Burnham Limestone, registered magnetic polarity assigned to the Matuyama reversed polarity chron, and so formed more than 0.78 My ago. The data for the Hallett Cove section is less clear.

5.1.2.2. Alunite and Halloysite

Alunite and halloysite occur in exposures of Plio-Pleistocene sediments in many localities around the margins of St Vincent Gulf but also in the underlying Cenozoic marine sequence (Crawford, 1965; Foster, 1974; Keeling & Hartley, 2005; Zang et al., 2006). In our study area, alunite seams in both the Robinson Point and Ngaltinga Formations are confined to the base of the succession in various locations, at or near the unconformity with underlying limestones (Figure 9). No alunite was recorded in central parts of the Willunga Embayment between Port Willunga and Sellicks Beach but halloysite was identified in the <2 µm particle size fraction of an Fe mega-mottled interval at the base of the Snapper Point Sand at Snapper Point (Figure 7).

In the Noarlunga Embayment, elongate lenses of alunite and rounded pods of halloysite occur in sands at the base of the Robinson Point Formation at Onkaparinga Trig (Figure 5) and between Moana and Witton Bluff (Supplement Figure 2.8). A 25 cm thick seam of alunite in basal Robinson Point Formation sands north of the jetty at Port Noarlunga extends continuously for several hundred metres and overlies green-yellow clays marking the top of the Eocene marine Blanche Point Formation. The underside of the seam is in sharp contact with the clays and displays rounded bulbous masses, up to 10 cm across, similar in form to load structures penetrating down into the underlying clays (Figure 8I). The upper surface of the seam is hummocky with irregular-shaped, convex-topped columns with the intervening depressions filled with sediment from the overlying unit. In the sections between Port Noarlunga and Witton Bluff there are up to three 1-5 cm conformable seams of alunite, 5-10 cm apart, in Robinson Point Formation sands. In the Seaford area, the base of the Robinson Point Formation consists of a relatively tough and compact fine sand that is impregnated with halloysite at the base but with lenses and discontinuous seams (up to 4 cm thick) of alunite above.

In the Willunga Embayment alunite and halloysite are less common. Halloysite is the dominant clay mineral in pink-red to yellow-green fine clayey sands in the basal 3-4 m of the Robinson Point Formation at Maslin Bay (Figure 4). Above are massive but discontinuous beds of white to grey sand with waxy pods (10-20 cm) of halloysite but uncommon alunite. Horizontal chalky lenses of alunite, several cm thick and up to 10 cm long, occur within the same interval. Just south of Chinaman Gully (Supplement Figure 2.3) discontinuous seams and elongate pods of alunite occur in a 20 cm-thick zone in green clays of the Ngaltinga Formation. The pods are up to 10 cm in diameter and, as at several other sites, have sharp lower contacts and diffuse upper contacts with surrounding clays. No halloysite was identified here. At Snapper Point, halloysite occurs in the clay fraction of a sample from approximately 10 m above the base of the Snapper Point Sand Member but alunite is not present.

The mineralogical compositions of samples of alunite and halloysite are detailed in Supplement Table 5.3. Based on XRD patterns, the alunite is close to end-member $KAl_3(S0_4)_2(OH)_6$ and well crystallised. Halloysite occurs in most samples. XRD peaks for halloysite are much broader and less intense than those for alunite and both 10 Å and 7 Å forms are present[3]. Interstratified clay minerals were not found in the clay fraction of samples containing halloysite but kaolinite and illite are present, although the latter is reduced in abundance. Jarosite and barite are other forms of sulphate alteration in the Plio-Pleistocene succession but were not identified in association with alunite (or halloysite).

Alunite and halloysite typically form in acid-sulphate environments (Keeling et al., 2010) and their co-existence in some sandy intervals in both the Robinson Point and Ngaltinga Formations at or near the base of the succession, just above the unconformity with Cenozoic marine sediments, is indicative of zones of groundwater seepage. These conditions were fundamentally different and more chemically aggressive than those producing the bleaching and Fe mega-mottling in sandy intervals higher in the sequence. It is likely that randomly interstratified clays and to a lesser extent illite were precursors for halloysite and/or kaolinite and provided the Al and K for alunite. Stable isotope ratios of alunites from the Noarlunga Embayment (Table 3) recorded negative δD values (-4 to -9) which were ascribed to evaporative concentration of solutes from meteoric waters in a regolith environment. The S-isotope composition of three samples (Bird et al., 1989; Table 3) is strongly positive ($+15.6^{o}/_{oo}$, $+17.7^{o}/_{oo}$, $+20.6^{o}/_{oo}$) and approaches that of modern seawater, indicating that the source of sulphate was most probably seawater that had been incorporated into the local groundwater via rainwater infiltration of aerosols from seacoasts (Dogramaci et al., 2001) located to the west–southwest.

[3] It is possible that at least some 7 Å halloysite formed by dehydration of the 10 Å form during storage in the laboratory prior to analysis.

Table 3. Isotopic analyses of alunite (Bird et al., 1989) from the Robinson Point Formation.

Sample	Location	Lat. Long.	Description	Total C (wt %)	Total H (wt %)	δD_{raw} $^{0}/_{00}$	$^{\#}\delta D_{corr}$ $^{0}/_{00}$	δ34S $^{0}/_{00}$	K (wt %)	40Ar (10^{-10} mol g^{-1})	40Ar (%)	Age (Ma) (±2δ)
RM142	Robinson Point Formation, 200m south of Onkaparinga Trig section.	35.15ºS 138.48ºE	White nodular alunite in green clay filling solutional hollow in Port Willunga Formation (Tertiary)	0.23	1.61	-5	-4±2	+15.5	8.560, 8.490	0.109	24.4	0.74±0.02
"RM208 - Same site as RM142	Robinson Point Formation, 200m south of Onkaparinga Trig section	34.97ºS 138.83ºE	White alunite from clay-filled hollow in Port Willunga Formation (Tertiary)	0.20	1.56	-10	-9±2	+17.7	8.760, 8.690	0.254	52	1.67±0.02
RM178	Robinson Point Formation, coastal cliffs, 1km south of Field River	35.08ºS 138.53ºE	Soft white alunite from thin bed	0.59	1.66	-11	-9±3	+20.6	8.228, 8.240	0.106	27.7	0.74±0.01

Ref: Bird et al. (1989); Bird et al. (1990)

$^{\#}\delta$D values corrected for H derived from organic matter & mineral contaminants

K-Ar analyses of alunite from two sites gave ages of around 0.74 My and 1.67 Ma at one site and around 0.74 My at the second (Bird et al., 1990; Table 3). The 1.67 Ma age was considered by Bird et al. (op. cit.) to have been the result of a small amount of admixed mica and so a minimum age of 740,000 years is likely.

6. Discussion

6.1. The question of an appropriate model

Our studies of the Plio-Pleistocene succession have identified lithological characteristics, with associated overprints relating to sediment accretion and maturation in fluvial-alluvial and pedogenic environments, as distinct from chemical alterations including Fe mega-mottling and bleaching and alunite-halloysite impregnation that post-date sedimentation. Here we review options for the environment and conditions that could have been active at these times (Figure 12).

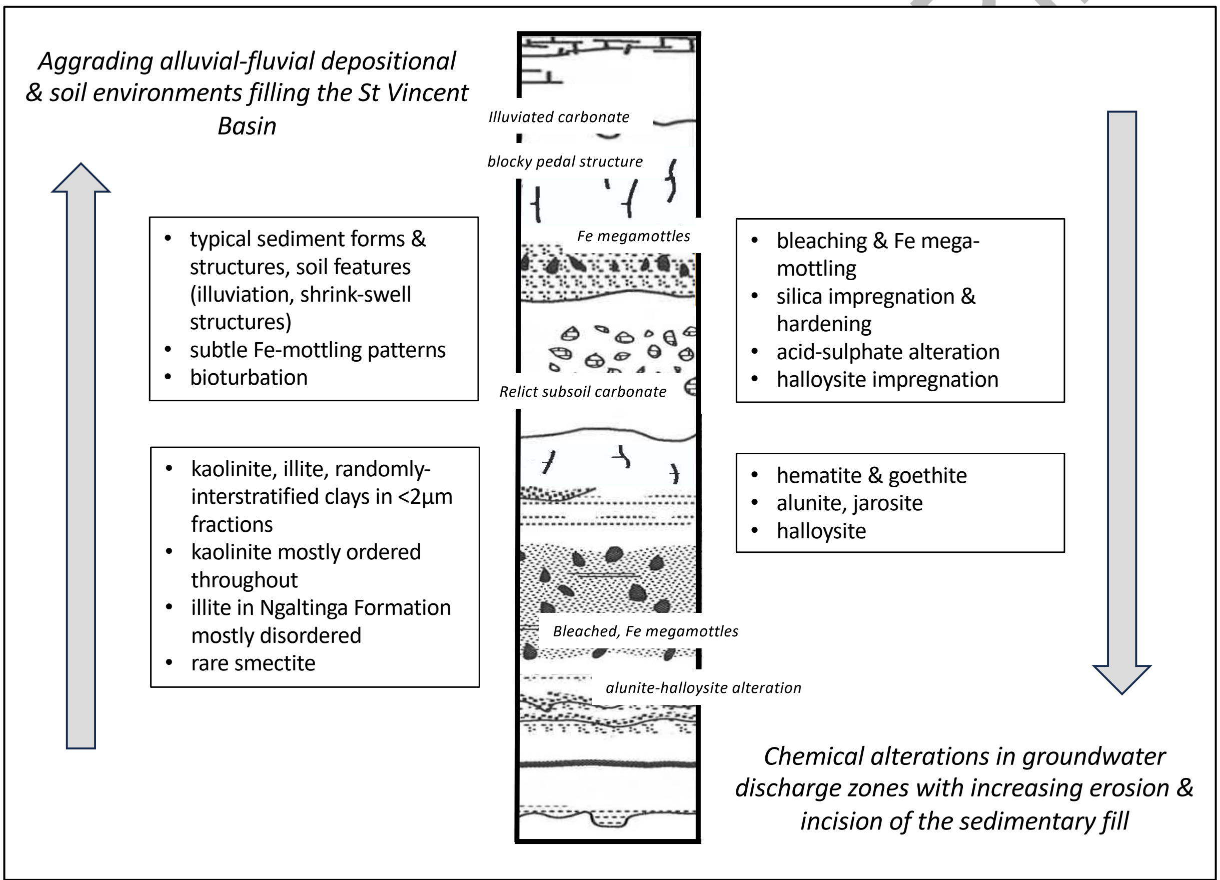

Figure 12. Schematic overview of the outcomes of this study of the Plio-Pleistocene succession.

Hematitic mega-mottles in intervals with significant bleaching and various degrees of induration by secondary silica are typical of sandy sediments in valleys or channels. They are not laterally extensive, occur at various levels in the stratigraphic sequence, and significantly post-date sedimentation. The hematite masses are typically bordered by networks of fractures marginal to which Fe (and other cations) have been leached and bleaching has resulted. None of several interpretations of the origin of Fe mega-mottles (Anand, 1998; Anand & Paine, 2002; Tonui, 1998) is a strong contender for the examples in our study area. One explanation might be that the mega-mottled intervals were zones in regolith environments through which acidic and somewhat reduced groundwaters seeped downgradient along the networks of fractures, progressively altering and leaching constituent minerals, whilst adjacent less-fractured and less-permeable zones retained (and possibly attracted the further precipitation of) hematite and goethite. As an indicator of the relatively low intensity of alteration, mica and feldspars persist in samples of bleached zones and Fe mottles (Table 2).

We have no evidence that the precursor sediments were uniformly iron-rich, although there are parts of some sections where exposures of sands are reddened by oxidation. As well, the mega-mottles don't have the form of accretionary structures but rather irregular masses with somewhat diffuse borders typical of dissolution. Some show evidence of cortical alteration to jarosite, which points to an acid-sulphate reaction post-dating the initial bleaching and reflects a different geochemical environment, albeit one in which groundwaters continued to seep through the interval along flowpaths dictated by the existing fracture network.

Although we are not confident about the detail of the mechanisms involved, there is a clear link with geomorphology and a flow-through of reactive acid groundwater, and we envisage places where local groundwaters discharged as springs or seeps from cliffs or valleysides incised into the succession. In this regard there are parallels with the geomorphology in parts of northern South Australia and the Paris Basin (France) in terms of relationships between groundwater silcretes and deep weathering during the dissection of plateau landscapes (Simon-Coinçon et al., 1996; Thiry et al., 2006; Thiry & Maréchal, 2001). It is of note that no bleached and mega-mottled intervals were observed by Sheard & Bowman (1994) in the same Plio-Pleistocene succession in the downfaulted Adelaide Plains Sub-Basin of the St Vincent Basin where there is no significant incision, and yet they are ubiquitous in the cliffed sections framing St Vincent Gulf.

We suggest that the alteration processes giving rise to alunite and halloysite in our study area were, like the bleaching and Fe mega-mottling, confined to zones where groundwaters (in this case acid-sulphate groundwaters) seeped from local aquifers. These zones generally occur just above the unconformity with the underlying marine limestones. As in the case of Fe mega-mottled intervals, such conditions did not exist in the same Plio-Pleistocene succession in the downfaulted Adelaide Plains Sub-Basin, and alunite and halloysite are not recorded there (Sheard & Bowman, 1994). The source of K for alunite is likely to have been the dissolution of illite and randomly interstratified illite-smectite in the precursor sediments: feldspar persists as a minor constituent of alunite/halloysite samples (Supplement Table 5.3). In the case of halloysitic intervals, the source materials are likely to have been randomly interstratified clays which are significantly depleted in comparison to their occurrence in adjacent unaltered sediments.

6.2. The timing of events

The Plio-Pleistocene succession in the study area does not contain index fossils and so depositional ages are difficult to establish. However, the Late Pliocene Burnham Limestone is intercalated with the basal part of the Robinson Point Formation and marks a final phase of marine environments in this area (Beu, 2017). From this time, in response to falling sea-levels, the whole of the St Vincent Basin was progressively traversed by a series of streams and alluvial fans and filled with sediments emanating from highlands on Fleurieu Peninsula in the east-northeast and Yorke Peninsula in the west (Figure 1). The Robinson Point Formation records the start of this cycle. In the upper parts of the overlying Ngaltinga Formation, a new source of aeolian sediment is recorded by remnants of carbonate palaeosols. This later became regionally dominant, accompanied by the onset of aridity, and resulted in a thick mantle of aeolian calcareous silt marking the cessation of fluvial deposition.

We don't know the timeframe for these depositional processes. However, the calcareous blanket has been linked to erosion by wind of the coastal calcareous sediments of the Bridgewater Formation along the southern margins of the continent (Milnes & Hutton, 1983; Daily et al., 1976; Milnes & Ludbrook, 1986; Milnes et al., 1987; Phillips, 1988; Phillips & Milnes, 1988; Milnes, 1992). Various ages for the earliest phases of the Bridgewater Formation range from >900 ka (Murray-Wallace, 2018) to 1.8 Ma (Orth, 1988; Beu, 2017). Thus, if the remant B_{Ca} horizons and aeolian calcareous blanket in the study area do herald the erosion of early parts of Bridgewater Formation, the underlying fluvial-alluvial sequence could be much older than this. The thickness and extent of the carbonate blanket, together with its many thick soil-generated calcrete horizons (Firman, 1969; Daily et al., 1976), is itself likely to have encompassed a significant time period marked by sedimentation interspersed with long intervals of pedogenesis.

A working hypothesis for evolution of the Plio-Pleistocene landscape in the St Vincent Basin is sketched out in Figure 13. Following deposition of the sedimentary fill, a prime trigger for erosional incision is falling sea-level. Other influences could have been movements on the fault-bounded margins of the basin (Stuart, 1969; Preiss, 2019b) and changing climate. We suggest that incision of the fill could have started at about the same time as the commencement of deposition of the aeolian carbonate blanket. The many significant fluctuations in sea-level from mid-Pleistocene times would have alternatively flooded the incised landscapes and then regressed, triggering further erosion and initiating the formation of the cliffed margins of the Gulf, which progressively retreated towards the eastern and western sides of the basin as sea-level rose after the last glacial maximum (Murray-Wallace et al., 2021). At times of relative stability of regional base level and local hydrology (Figure 13B - D), significant alteration occurred in zones of local groundwater outflow according to the geochemical environment: thus the formation of bleached and Fe mega-mottled zones when seepage waters were acidic and somewhat reduced, and alunite-halloysite when seepage waters had an acid-sulphate composition. This progression implies that the Fe mega-mottled intervals highest in the succession are the oldest 'fossil' features of the landscape and that the alunite-halloysite alteration is youngest, matching proximity to the periods of relative stability of the phreatic surface which followed systematic falls in regional base level. More detailed geochronological data is clearly required but this matches the information we have for regolith weathering and alteration features elsewhere (Bird et al., 1990; Vasconcelas & Conroy, 2003; Heim et al., 2006; Morris 2015; Chivas & Bourman, 2018).

7. Summary

Thick exposures of Plio-Pleistocene non-marine sediments in modern seacliffs fronting the down-faulted Noarlunga and Willunga Embayments in eastern parts of the St Vincent Basin include a basal fluvial and alluvial sequence, an intermediate thick and extensive clay unit topped with fluvial sands, and an uppermost blanket of aeolian carbonate silt and pedogenic calcretes. Lithological and mineralogical details in four key sections and eight subsidiary sections characterise the sediments in the succession and provide the basis for distinguishing syn-depositional from significantly post-depositional overprints, both physical and chemical, the latter in regolith environments. A model is proposed to account for the non-marine sedimentary infilling of the embayments being succeeded by erosional incision and chemical alteration triggered by the interception and seepage discharge of local groundwater aquifers. The timing of these events in the history of the landscape is not yet clear.

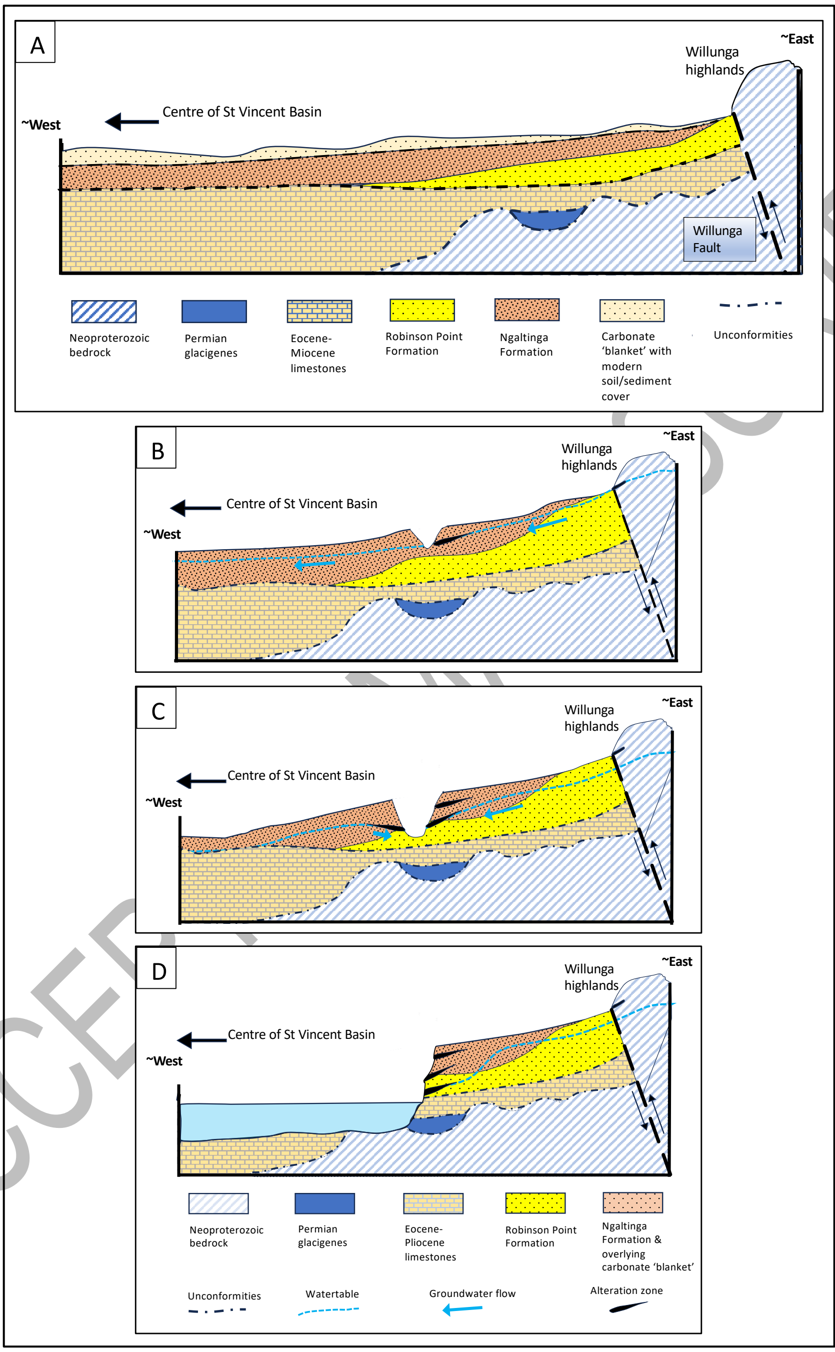

Figure 13. Schematic showing original disposition of the Plio-Pleistocene succession in the Noarlunga and Willunga Embayments (A) and subsequence stages in the erosion and incision of the sequence following falls in regional base level and local watertable levels (B, C, D). At each stage, significant geochemical alteration occurred in zones of local groundwater outflow. Note that 'Eocene-Pliocene' includes Hallett Cove Sandstone whilst 'Robinson Point Formation' includes Burnham Limestone.

8. Acknowledgements

The contributions of many colleagues are gratefully acknowledged for initially supervising and advising these studies and for later discussions about the hypotheses raised in our explanation of the observations and data. In particular, Prof. Malcolm Oades (Soil Science, University of Adelaide), Dr Keith Norrish and John Pickering (CSIRO Soils), Prof. Bob Gilkes (Soils & Agriculture, University of Western Australia) and Dr Marjorie Muir (CRA Exploration) provided help and encouragement during early phases of the project, together with PhD colleagues Bob Bourman and Sally Phillips. Dr Medard Thiry, Prof. Bob Bourman, Dr Wolfgang Preiss, Prof. Colin Murray-Wallace and Dr Phil Plummer discussed early versions of the ms with us. We are particularly grateful for the advice from Editor Dr Murray Gingras and reviewer Dr Mario Werner (Geological Survey of South Australia).

9. Author contributions

Richard May was awarded a PhD for the project and overviewed the preparation of the ms. **Anthony Milnes** co-supervised the PhD investigation and prepared the ms.

10. Data availability statement

Supplementary data are available at https://doi.org/10.6084/m9.figshare.25951666

11. Declaration of Competing Interest

The authors declare that they have no known competing financial interests or personal relationships that could have appeared to influence the work reported in this paper.

12. References

Aldam, R., Fairbairn, W. A., Preiss, W. V. & Olliver, J. G. (2022). Geology of the McLaren Vale Wine Region. McLaren Vale Grape & Wine Tourist Association brochure.

Anand, R. R. (1998). Distribution, classification and evolution of ferruginous materials over greenstones in the Yilgarn Craton – implications for mineral exploration. *In* Eggleton, R. A. (Ed). The State of the Regolith. Geological Society of Australia Special Publication 20: 175-193. ISBN 1 876315 07 5

Anand, R. R. & Paine, M. (2002). Regolith geology of the Yilgarn Craton, Western Australia: implications for exploration. Australian Journal of Earth Sciences 49, 3–162. https://doi.org/10.1046/j.1440-0952.2002.00912.x

Beu, J. G. (2017). Evolution of *Janthina* and *Recluzia* (Mollusca: Gastropoda: Epitoniidae). Records of the Australian Museum 69(3), 119–222. ISSN 0067-1975 (print), ISSN 2201-4349 (online). https://doi.org/10.3853/j.2201-4349.69.2017.1666

Bird, M. I., Andrew, A.S., Chivas, A. R. & Lock, D. E. (1989). An isotopic study of surficial alunite in Australia: 1. Hydrogen and sulphur isotopes. Geochimica Cosmochimica Acta 53, 3223-3237. https://doi.org/10.1016/0016-7037(89)90103-8

Bird, M. I., Chivas, A. R. & McDougall, I. (1990). An isotopic study of surficial alunite in Australia. 2. Potassium-argon geochronology. Chemical Geology (Isotope Geoscience Section) 80, 133-145. https://doi.org/10.1016/0168-9622(90)90022-5

Bourman, R. P., Barnett, S., Murray-Wallace, C., Buckman, S., Banerjee, D. & Panda, D. (2022). A stratigraphic revision of the Pleistocene succession in the Noarlunga and Willunga Embayments, South Australia. MESA Journal 96, 27-36.

Bye, J. A. T. & Kampf, J. (2008). Physical Oceanography. *In* (Eds Shepherd, S. A., Bryers, S., Kirkegaard, I., Harbison, P. & Jennings. J. T.) Natural History of Gulf St Vincent, Chapter 5, pp 56-70. (Royal Society of South Australia).

Chivas, A. R. & Bourman, R. P. (2018). Oxygen isotope dating the Australian regolith: A review and new applications. *In* Krapf C., Keeling, J. & Petts, A. (Eds). Proceedings for 5th Australian Regolith Geoscientists Association Conference, Wallaroo, South Australia, Report Book 2018/00011, 41-42. (Department of the Premier and Cabinet, South Australia, Adelaide).

Cooper, B. J. (1985). The Cainozoic St Vincent Basin – tectonics, structure, stratigraphy. *In* (Ed. J. M. Lindsay). ‘Stratigraphy, Palaeontology, Malacology: Papers in Honour of Dr Nell Ludbrook’. South Australian Department of Mines and Energy. Special Publication 5, 35-49.

Crawford, A. R. (1965). The geology of Yorke Peninsula. South Australia Geological Survey Bulletin 39, 62pp.

Daily, B., Firman, J. B., Forbes, B. G. & Lindsay, J. M. (1976). Geology. *In* (Eds Twidale, C. R., Tyler, M. J. & Webb, B. P.) Natural History of South Australia, Chapter 1, pp 5-42. (Royal Society of South Australia). ISBN 0 9596627 0 7

Dogramaci, S. S., Herczeg, AL, Schi, S. L. & Bone, Y. (2001). Controls on δ^{34}S and δ^{18}O of dissolved sulfate in aquifers of the Murray Basin, Australia and their use as indicators of flow processes. Applied Geochemistry 16, 475-488. https://doi.org/10.1016/S0883-2927(00)00052-4

Firman, J. B. (1966). Stratigraphic units of Late Cainozoic Age in the Adelaide Plains Basin, South Australia. Quarterly Geological Notes, Geological Survey of South Australia 17, 6-9.

Firman, J. B. (1969). Stratigraphy and landscape relations of soil materials near Adelaide, South Australia. Transactions of the Royal Society of South Australia 93, 39-54. https://www.biodiversitylibrary.org/item/127593

Forbes, B. G. (Compiler) (1983) Noarlunga map sheet, Geological Atlas of South Australia, I:50 000 Series. Geological Survey of South Australia.

Foster, C. B. (1974). Stratigraphy and palynology of the Permian at Waterloo Bay, Yorke Peninsula, South Australia. Transactions of the Royal Society of South Australia 98, 29-42. https://www.biodiversitylibrary.org/item/127779

Glaessner, M. F. & Wade, M. (1958). The St Vincent Basin. Journal of the Geological Society of Australia 5, 115-126.

Hampton, M. A., Griggs, G. B., Edil, T. B., Guy, D. E., Kelley, J. T., Komar, P. D., Mickelson, D. M. & Shipman, H. M. (2004). Processes that govern the formation and evolution of coastal cliffs. *In* (Eds Hampton, M. A. & Griggs, G. B.) Formation, Evolution, and Stability of Coastal Cliffs–Status and Trends. US Geological Survey Professional Paper 1693, 1-4. http://pubs.usgs.gov/pp/pp1693/

Heim, J. A., Vasconcelos, P. M., Shuster, D. L., Farley, K. A. & Broadbent, G. (2006). Dating paleochannel iron ore by (U-Th/He analysis of supergene goethite, Hamersley Province, Australia. Geology 34(3), 173-176. https://doi.org/10.1130/G22003.1

Keeling, J. L. & Hartley, K. L. (2005). Poona and Wheal Hughes Cu deposits, Moonta, South Australia. 3pp. *In* (Eds C.R.M. Butt, I.D.M. Robertson, K.M. Scott, M. Cornelius) Regolith Expression of Australian Ore Systems. CRC LEME. ISBN 1921039280

Keeling, J. L., Self, P. G. & Raven, M. D. (2010). Halloysite in Cenozoic sediments along the Eucla Basin margin. MESA Journal 59, 24-28.

Ludbrook, N. H. (1983). Molluscan faunas of the Early Pleistocene Point Ellen Formation and Burnham Limestone, South Australia. Transactions of the Royal Society of South Australia 107, 37–49. https://www.biodiversitylibrary.org/bibliography/168319

McArthur, W. M. & Bettenay, E. (1974). The development and distribution of the soils of the Swan coastal plain, Western Australia. Soil Publication 16, CSIRO Australia. ISBN 0643001085

McGowran, B. & Alley, N. F. (2008). History of the Cenozoic St Vincent Basin in South Australia. *In* (Eds Shepherd, S. A., Bryers, S., Kirkegaard, I., Harbison, P. & Jennings. J. T.) Natural History of Gulf St Vincent, Chapter 2, pp 13-28. (Royal Society of South Australia).

McGowran, B., Lemon, N., Preiss, W. & Olliver, J. (2016). Cenozoic Willunga Embayment: from Australo-Antarctic Gulf to Sprigg Orogeny. Geological Field Excursion Guide, Australian Earth Sciences Convention, 48pp. Department of State Development, South Australia.

May, R. I. (1992). Origin, mineralogy and diagenesis of sediments from the Noarlunga and Willunga Embayments, South Australia. PhD thesis, University of Adelaide. https://digital.library.adelaide.edu.au/dspace/handle/2440/19746

Meyer, R. & Pena Dos Reis, R. B. (1985). Paleosols and alunite silcretes in continental Cenozoic of western Portugal. Journal of Sedimentary Petrology 55, 76-85. https://doi.org/10.1306/212F8616-2B24-11D7-8648000102C1865D

Milnes, A. R. (1992). Calcrete. *In* (Eds) Martini, I. P. & Chesworth, W. Weathering, Soils & Paleosols. Ch. 13, 309-347. (Elsevier: Amsterdam). ISBN 0-444-89198-6

Milnes, A. R. & Hutton, J. T. (1983). Calcretes in Australia – a review. In Soils: an Australian Viewpoint, Chapter 10, 119-162. (CSIRO, Melbourne/Academic Press, London). ISBN 0 643 00400 9

Milnes, A. R., Kimber, R. W. & Phillips, S. E. (1987). Studies in calcareous aeolian landscapes of southern Australia. *In* Liu, Tungsheng (editor-in-chief). Aspects of Loess Research, 130-139. (China Ocean Press: Beijing). ISBN 7-5027-0050-1

Milnes, A. R. & Ludbrook, N. H. (1986). Provenance of microfossils in aeolian calcarenites and calcretes in southern South Australia. Australian Journal of Earth Sciences 33, 145-159. https://doi.org/10.1080/08120098608729356

Morris, B. J. (2015). Coober Pedy Precious Stones Field: $^{40}Ar/^{39}Ar$ geochronology of alunite and opal formation. Report Book 2015/00007, 29pp (Department of State Development, South Australia, Adelaide).

Murray-Wallace, C. V. (2018). Quaternary History of the Coorong Coastal Plain, Southern Australia: an archive of environmental and global sea level changes. (Springer International Publishing). 229pp. https://doi.org/10.1007/978-3-319-89342-6

Murray-Wallace, C. V., Cann, J. H., Yokoyama, Y., Nicholas, W. A., Lachlan, T. J., Pan, T-Y., Dosetto, A., Belperio, A. P. & Gostin, V. A. (2021). Late Pleistocene interstadial sea-levels (MIS 5a) in Gulf St Vincent, southern Australia, constrained by amino acid racemization dating of the benthic foraminifer *Elphidium macelliforme*. Science Reviews 259, 106899. https://doi.org/10.1016/j.quascirev.2021.106899

Orth, K. (1988). Geology of the Warrnambool 1:50 000 map. Geological Survey Report No. 86. (Department of Industry, Technology and Resources, Victoria).

Phillips, S. E. (1988). The interaction of geological, geomorphic and pedogenic processes in the genesis of calcrete. PhD thesis, University of Adelaide. https://digital.library.adelaide.edu.au/dspace/handle/2440/19052

Phillips, S. E. & Milnes, A. R. (1988). The Pleistocene terrestrial carbonate mantle on the southeastern margin of the St Vincent Basin, South Australia. Australian Journal of Earth Sciences 35, 463-481. https://doi.org/10.1080/08120098808729463

Pillans, B. & Bourman, R. (1996). The Brunhes/Matuyama Polarity Transition (0.78 Ma) as a chronostratigraphic marker in Australian regolith studies. AGSO Journal of Australian Geology & Geophysics 16, 289-294.

Pillans, B. & Bourman, R. (2001). Mid Pleistocene arid shift in southern Australia, dated by magnetostratigraphy. Australian Journal of Soil Research 39, 89-98. https://doi:10.1071/sr99089

Plink-Björklund (2021). Distributive Fluvial Systems: Fluvial and Alluvial Fans. Encyclopedia of Geology (2nd edn), 745-758. https://doi.org/10.1016/B978-0-08-102908-4.00015-1

Preiss, W. V. (2019a). A new geological map of Hallett Cove. MESA Journal 91, 33-50.

Preiss, W. V. (2019b). The tectonic history of Adelaide's scarp-forming faults. Australian Journal of Earth Sciences 66, 305-365. https://doi.org/10.1080/08120099.2018.1546228

Retallack, G. J. (1988). Field recognition of paleosols. *In* (Eds) Reinhardt, J. & Sigleo, W. R. Paleosols and weathering through geologic time: princíples and applications. Geological Society of America Special Paper 216, 1-20. https://doi:10.1130/spe216-p1

Richardson, L., Mathews, E. & Hesp, A. (2005). Geomorphology and sedimentology of the South Western Planning Area of Australia. Geoscience Australia Record 2005/17, 138pp. ISBN: 1 920871 56 X

Schwertmann, U. & Taylor, R. M. (1989). Iron oxides. *In* (Eds) Dixon, J. B. & Weed, S. E. *Minerals in Soil Envíronments* (2nd ed.), Soil Science Society of America, Madison, WI, 379-438. ISBN 0-89118-787-1

Sheard, M. J. & Bowman, G. M. (1987a). Definition of the Keswick Clay, Adelaide/Golden Gove Embayment, Para and Eden Blocks, South Australia. Quarterly Geological Notes, Geological Survey of South Australia 103, 4-9.

Sheard, M. J. & Bowman, G. M. (1987b). Definition of the upper boundary of the Hindmarsh Clay, Adelaide Plains sub-Basin and Adelaide/ Golden Gove Embayment. Quarterly Geological Notes, Geological Survey of South Australia 103, 9-16.

Sheard, M. J. & Bowman, G. M. (1994). Soils, stratigraphy and engineering geology of near surface materials of the Adelaide Plains. Report Book 94/9, Vol 1. Department of Mines and Energy, South Australia.

Sheard, M. J., Bowman, G. M., Wade, C. E. & Phillips, S. E. (2015). Modbury North Catena Study in metropolitan Adelaide: geology, regolith, soils and gilgai; their mineralogy, geochemistry, landscape evolution, geomechanics, and implications for civil engineering. Report Book 2015/00028. Department of Mines and Energy, South Australia.

Simon-Coinçon, R., Milnes, A. R., Thiry, M, & Wright, M. J. (1996). Evolution of landscapes in northern South Australia in relation to the distribution and formation of silcretes. Journal of the Geological Society London 153, 467-480. https://doi.org/10.1144/gsjgs.153.3.0467

Stuart, W. J. (1969). Stratigraphic and structural development of the St Vincent Tertiary Basin, South Australia. PhD Thesis, University of Adelaide. https://digital.library.adelaide.edu.au/dspace/handle/2440/21275

Thiry, M. & Maréchal, B. (2001). Development of tightly cemented sandstone lenses within uncemented sand: Example of the Fontainebleau Sand (Oligocene) in the Paris Basin. Journal of Sedimentary Research, 71, 473-483. https://doi.org/10.1306/2dc40956-0e47-11d7-8643000102c1865d

Thiry, M., Milnes, A. R., Rayot, V. & Simon-Coinçon, R. (2006). Interpretation of palaeoweathering features and successive silicifications in the Tertiary regolith of inland Australia. Journal of the Geological Society London 163, 723-736. https://doi:10.1144/0014-764905-020

Tonui, E. K. (1998). Regolith mineralogy and geochemistry at Goonumbla, Parkes, NSW. PhD thesis, Australian National University. http://hdl.handle.net/1885/144604

Vasconcelos, P. M. & Conroy, M. (2003). Geochronology of weathering and landscape evolution, Dugald River valley, NW Queensland, Australia. Geochimica et Cosmochimica Acta 67, 2913–2930. https://doi.org/10.1016/S0016-7037(02)01372-8

Ventra, D. & Clarke, L.E. (2018). Geology and geomorphology of alluvial and fluvial fans: current progress and research perspectives. *In* Ventra, D. & Clarke, L.E. (eds) Geology and Geomorphology of Alluvial and Fluvial Fans: Terrestrial and Planetary Perspectives. Geological Society, London, Special Publications, 440. https://doi.org/10.1144/SP440.16

Von Der Borch, C. C. & Lock, D. (1979). Geological significance of Coorong dolomites. Sedimentology 26, 813-824. https://doi.org/10.1111/j.1365-3091.1979.tb00974.x

Ward, W. T. (1966). Geology, geomorphology and soils of the south-western part of county Adelaide, South Australia. Soil Publication 23, 115p. (CSIRO Australia). ISBN 0 643 04209 1

Zang, W., Cowley, W. M. & Fairclough, M. C. (2006). Maitland Special, South Australia. 1:250 000 Geological Series – Explanatory Notes. 62pp. Geological Survey of South Australia. ISBN 0 7590 1380 2

